Machine Learning Panel Data Regressions with Heavy-tailed Dependent Data: Theory and Application

Andrii Babii* Ryan T. Ball† Eric Ghysels‡ Jonas Striaukas§

June 18, 2022

Abstract

The paper introduces structured machine learning regressions for heavy-tailed dependent panel data potentially sampled at different frequencies. We focus on the sparse-group LASSO regularization. This type of regularization can take advantage of the mixed frequency time series panel data structures and improve the quality of the estimates. We obtain oracle inequalities for the pooled and fixed effects sparse-group LASSO panel data estimators recognizing that financial and economic data can have fat tails. To that end, we leverage on a new Fuk-Nagaev concentration inequality for panel data consisting of heavy-tailed τ-mixing processes.

Keywords: High-dimensional panels, large N and T panels, mixed-frequency data, sparse-group LASSO, fat tails.

*University of North Carolina at Chapel Hill - Gardner Hall, CB 3305 Chapel Hill, NC 27599-3305. Email: babii.andrii@gmail.com.

†Stephen M. Ross School of Business, University of Michigan, 701 Tappan Street, Ann Arbor, MI 48109. Email: rtball@umich.edu.

‡Department of Economics and Kenan-Flagler Business School, University of North Carolina–Chapel Hill. Email: eghysels@unc.edu.

§LIDAM UC Louvain and FRS-FNRS Research Fellow. Email: jonas.striaukas@gmail.com.

1 Introduction

We analyze panel data regressions in a high-dimensional setting where the number of time-varying covariates can be very large and potentially exceed the sample size. We leverage on the structured sparsity approach using sparse-group LASSO (sg-LASSO) regularization for time series data with dictionaries. The advantages of this approach for individual time series data, potentially sampled at mixed frequencies, have been recently reported in Babii, Ghysels, and Striaukas (2022b), who focus on nowcasting the US GDP growth in a data-rich environment. In this paper, we first show how to leverage on the sparse group regularization in a panel data setting. Second, we study the benefits of using the cross-sectional dimension for prediction with panel data paying particular attention to the issues of fat-tailed series which are relevant for the application involving financial time series. Third, we develop the debiased heteroskedasticity autocorrelation consistent (HAC) inference for regularized panel data regressions. Lastly, we provide an illustrative empirical example involving systematically predictable errors in analysts with individual firm earnings forecasts.

Our paper relates to the literature on high-dimensional panel data models and the LASSO regularization; see Harding and Lamarche (2019), Chiang, Rodrigue, and Sasaki (2019), Chernozhukov, Hausman, and Newey (2019), Belloni, Chen, Padilla, et al. (2019), Belloni, Chernozhukov, Hansen, and Kozbur (2016), Lu and Su (2016), Kock (2016), Su, Shi, and Phillips (2016), Farrell (2015), Kock (2013), Lamarche (2010), Koenker (2004), among others.

It is worth emphasizing what sets our paper apart from the existing literature. An applied researcher facing high-dimensional panel data has several modeling decisions to make. Should (s)he simply run single regularized regression models, or take advantage of the cross-sectional dimension on the panel? If the latter is the case, how should one proceed? Pool the regressions or consider a fixed effect panel model to capture cross-sectional heterogeneity?

Note that there are a lot of subtleties involved. Take for example the decision to run individual regularized time series regressions versus pooled or fixed effect panel regressions. In a high-dimensional setting, it is not simply a matter of replacing T by NT to account for the panel data environment. In the fixed effect panel model we pay price for estimating N fixed effects which plays a role similar to the effective dimension of covariates. In a pooled panel model, we do not incur this penalty, but is pooling warranted? What about simply ignoring the panel structure? If we add to the model choice also the fact that the data are not sampled at the same frecquency — a situation often encountered in many high-dimensional prediction problems — then we also need to make a choice on how to approach parameter proliferation

and regularization in terms of the MIDAS parameterization (e.g. UMIDAS as in Foroni, Marcellino, and Schumacher (2015) or constrained polynomials as in Babii, Ghysels, and Striaukas (2022b)). Moreover, the existing literature relates mostly to the microeconometric problems and does not address comprehensively (1) the advantages of long panels; (2) the performance of regularized panel data estimators with potentially heavy-tailed covariates and regression errors, (3) the debiased HAC inference for regularized panel data, and (4) the sg-LASSO regularization of Simon, Friedman, Hastie, and Tibshirani (2013) in a panel data setting.

In this paper we provide the theoretical underpinnings for all the aforementioned issues an applied researcher faces, report on Monte Carlo simulations to gauge the finite sample behavior of the various estimation methods and finally include an empirical application which provides new insights on potential inefficiencies and biases in earnings forecasting by analysts.

Our theory recognizes that the economic and financial time series data are often persistent with fat tails. To that end, we develop new Fuk-Nagaev and Rosenthal's inequalities and the central limit theorem for long τ-mixing panel.[1] Using new results, we obtain the oracle inequalities for the sg-LASSO that shed new light on how the predictive performance of pooled and fixed effect estimators scales with N (cross-section) and T (time series). Additionally, we present the powerful debiased inferential methods for the regularized long panel data. The supporting theoretical results imply that the standard errors and the length of confidence intervals scale at the $O(1/\sqrt{NT})$ rate instead of the $O(1/\sqrt{N})$ rate that we typically encounter for fixed T approximations or the $O(1/\sqrt{T})$ rate for the individual time series regressions considered in Babii, Ghysels, and Striaukas (2022b).

In this way we also contribute to the modern panel data literature, where both N and T can be large; see Fernández-Val and Weidner (2016), Hansen (2007), Alvarez and Arellano (2003), Hahn and Kuersteiner (2002), and Phillips and Moon (1999), among others. In contrast to this literature, we focus on the high-dimensional panels and our theory covers the regularized regression including the LASSO, the group-LASSO, and the sparse-group LASSO estimators.

The theory is extensively supported by the Monte Carlo experiments, where we focus on the debiased inference in the high-dimensional panel data and find that the individual regressions feature worse performance compared to the pooled regressions, hence, showing the usefulness of pooling the data. The results of these experiments

[1] It is worth mentioning that the direct application of the theory developed in Babii, Ghysels, and Striaukas (2022a,b) for single time series regression models leads to inferior results for heavy-tailed panel data.

also indicate that the structured regularization leads to better Granger causality tests in small samples.

In our empirical application we revisit a topic raised by Ball and Ghysels (2018) and Carabias (2018), but not resolved via formal inference in a high-dimensional setting. Namely, their empirical findings suggest that analysts tend to focus on their firm/industry when making earnings predictions while not fully taking into account the macroeconomic events affecting their firm/industry. More broadly, Ball and Ghysels (2018) argue that analysts do not fully exploit information embedded in high-dimensional data and therefore *leave money on the table*. Thanks to the theoretical contributions in the current paper we can formally test that hypothesis in a data-rich environment. Note that, as Ball and Ghysels (2018) point out, it is important to take into account the mixed frequency nature of the data flow, which is why the machine learning panel regression methods presented in the paper apply to mixed frequency data. We use 26 predictors, including traditional macro and financial series as well as non-standard series generated by textual analysis of financial news. Using such a rich set of covariates, we test whether analyst's consensus earnings prediction errors are systematically related to either one of the aforementioned variables.

The paper is organized as follows. Section 2 introduces the models and estimators. Oracle inequalities for sg-LASSO panel data regressions appear in Section 3. Section 4 develops the debiased HAC inference for regularized panel data regressions. Monte Carlo simulations are reported in Section 5. The results of our empirical application are reported in Section 6. Section 7 concludes. All technical details and detailed data descriptions appear in the Appendix and the Online Appendix.

Notation: For a random variable $X \in \mathbf{R}$, let $\|X\|_q = (\mathbb{E}|X|^q)^{1/q}$ be its L_q norm with $q \geq 1$. For $p \in \mathbf{N}$, put $[p] = \{1, 2, \ldots, p\}$. For a vector $\Delta \in \mathbf{R}^p$ and a subset $J \subset [p]$, let Δ_J be a vector in $\mathbf{R}^p$ with the same coordinates as Δ on J and zero coordinates on J^c. Let $\mathcal{G}$ be a partition of $[p]$ defining the group structure, which is assumed to be known to the econometrician. For a vector $\beta \in \mathbf{R}^p$, the sparse-group structure is described by a pair $(S_0, \mathcal{G}_0)$, where $S_0 = \{j \in [p] : \beta_j \neq 0\}$ and $\mathcal{G}_0 = \{G \in \mathcal{G} : \beta_G \neq 0\}$ are the support and respectively the group support of β.

We also use $|S|$ to denote the cardinality of a set S. For $b \in \mathbf{R}^p$, its ℓ_q norm is denoted as $|b|_q = (\sum_{j\in[p]} |b_j|^q)^{1/q}$ if $q \in [1, \infty)$ and $|b|_\infty = \max_{j\in[p]} |b_j|$ if $q = \infty$. For a group structure $\mathcal{G}$, the $\ell_{2,1}$ group norm of $b \in \mathbf{R}^p$ is defined as $\|b\|_{2,1} = \sum_{G\in\mathcal{G}} |b_G|_2$. For $\mathbf{u}, \mathbf{v} \in \mathbf{R}^J$, the empirical inner product is defined as $\langle \mathbf{u}, \mathbf{v} \rangle_J = J^{-1} \sum_{j=1}^J u_j v_j$ with the induced empirical norm $\|.\|_J^2 = \langle ., . \rangle_J = |.|_2^2/J$. For a symmetric $p \times p$ matrix A, let $\text{vech}(A) \in \mathbf{R}^{p(p+1)/2}$ be its vectorization consisting of the lower triangular and the

diagonal elements. Let A_G be a sub-matrix consisting of rows of A corresponding to indices in $G \subset [p]$. If $G = \{j\}$ for some $j \in [p]$, then we simply write $A_G = A_j$. Let $\|A\|_\infty = \max_{j\in[p]} |A_j|$ be the matrix norm. For $a, b \in \mathbf{R}$, we put $a \vee b = \max\{a, b\}$ and $a \wedge b = \min\{a, b\}$. Lastly, we write $a_n \lesssim b_n$ if there exists a (sufficiently large) absolute constant C such that $a_n \leq Cb_n$ for all $n \geq 1$ and $a_n \sim b_n$ if $a_n \lesssim b_n$ and $b_n \lesssim a_n$.

2 High-dimensional (mixed frequency) panels

Motivated by our empirical application, we allow the high-dimensional set of predictors to be sampled at a higher frequency than the target variable. Let K be the total number of time-varying predictors $\{x_{i,t-(j-1)/m,k} : i \in [N], t \in [T], j \in [m], k \in [K]\}$ possibly measured at some higher frequency with m observations for every low-frequency period $t \in [T]$ and every entity $i \in [N]$. Consider the following (mixed frequency) panel data regression

$$y_{i,t+h} = \alpha_i + \sum_{k=1}^{K} \psi(L^{1/m}; \beta_k) x_{i,t,k} + u_{i,t},$$

where $h \geq 0$ is the prediction horizon, α_i is the entity-specific intercept, and

$$\psi(L^{1/m}; \beta_k) x_{i,t,k} = \frac{1}{m} \sum_{j=1}^{m} \beta_{j,k} x_{i,t-(j-1)/m,k} \tag{1}$$

is a high-frequency lag polynomial with $\beta_k = (\beta_{1,k}, \ldots, \beta_{m,k})^\top \in \mathbf{R}^m$. More generally, the frequency can also be specific to the predictor $k \in [K]$, in which case we would have m_k instead of m. We can also absorb the (low-frequency) lags of $y_{i,t}$ in the set of covariates. When $m = 1$, we retain the standard (dynamic if we include lagged dependent variables) panel data regression model

$$y_{i,t+h} = \alpha_i + \sum_{k=1}^{K} \beta_k x_{i,t,k} + u_{i,t},$$

while $m > 1$ signifies that the high-frequency lags of $x_{i,t,k}$ are also included. The large number of predictors K with potentially large number of high-frequency measurements m can be a rich source of predictive information, yet at the same time, estimating $N + m \times K$ parameters is costly and may reduce the predictive performance in small samples.

2.1 Dealing with mixed frequency panel data

To reduce the proliferation of lag parameters, we follow the MIDAS literature; see Ghysels, Santa-Clara, and Valkanov (2006), Ghysels, Sinko, and Valkanov (2006), and Babii, Ghysels, and Striaukas (2022a,b). Instead of estimating m individual slopes of high-frequency covariate $k \in [K]$ in equation (1), with some abuse of notation, we estimate a weight function ω parameterized by $\beta_k \in \mathbf{R}^L$ with $L < m$

$$\psi(L^{1/m}; \beta_k) x_{i,t,k} = \frac{1}{m} \sum_{j=1}^{m} \omega\left(\frac{j-1}{m}; \beta_k\right) x_{i,t-(j-1)/m,k},$$

where

$$\omega(s; \beta_k) = \sum_{l=0}^{L-1} \beta_{l,k} w_l(s), \qquad \forall s \in [0,1]$$

and $(w_l)_{l \geq 0}$ is a collection of L approximating functions, called the *dictionary* in the machine learning literature. An example of a dictionary is the set of orthogonal Legendre polynomials on $[0,1]$ that can be computed via the Rodrigues' formula $w_l(s) = \frac{1}{l!} \frac{\mathrm{d}^l}{\mathrm{d}s^l}(s^2 - s)^l$.[2] For instance, the first five elements are

$$\begin{aligned}
w_0(s) &= 1 \\
w_1(s) &= 2s - 1 \\
w_2(s) &= 6s^2 - 6s + 1 \\
w_3(s) &= 20s^3 - 30s^2 + 12s - 1 \\
w_4(s) &= 70s^4 - 140s^3 + 90s^2 - 20s + 1.
\end{aligned}$$

More generally, we can use Gegenbauer polynomials, trigonometric polynomials, or wavelets. The orthogonal polynomials usually have better numerical properties than their popular non-orthogonal counterpart, such as the Almon (1965) lag structure. The attractive feature of linear in parameters dictionaries is that we can map the MIDAS regression to the linear regression framework that can be solved via a convex optimization. To that end, define $\mathbf{x}_i = (X_{i,1}W, \ldots, X_{i,K}W)$, where for each $k \in [K]$, $X_{i,k} = (x_{i,t-(j-1)/m,k})_{t \in [T], j \in [m]}$ is a $T \times m$ matrix of predictors and $W = (w_l((j-1)/m)/m)_{j \in [m], 0 \leq l \leq L-1}$ is an $m \times L$ matrix corresponding to the dictionary $(w_l)_{l \geq 0}$. In

[2]The Legendre polynomials have the universal approximation property and can approximate any continuous function uniformly on $[0,1]$. At the same time they can generate a rich family of MIDAS weights with a relatively small number of parameters which is attractive in time series applications where the signal-to-noise ratio is often low.

addition, let $\mathbf{y}_i = (y_{i,1+h}, \ldots, y_{i,T+h})^\top$ and $\mathbf{u}_i = (u_{i,1}, \ldots, u_{i,T})^\top$. Then the regression equation after stacking time series observations for each $i \in [N]$ is

$$\mathbf{y}_i = \iota\alpha_i + \mathbf{x}_i\beta + \mathbf{u}_i,$$

where $\iota \in \mathbf{R}^T$ is the all-ones vector and $\beta \in \mathbf{R}^{LK}$ is a vector of slopes. Lastly, put $\mathbf{y} = (\mathbf{y}_1^\top, \ldots, \mathbf{y}_N^\top)^\top$, $\mathbf{X} = (\mathbf{x}_1^\top, \ldots, \mathbf{x}_N^\top)^\top$, and $\mathbf{u} = (\mathbf{u}_1^\top, \ldots, \mathbf{u}_N^\top)^\top$. Then the regression equation after stacking all cross-sectional observations is

$$\mathbf{y} = B\alpha + \mathbf{X}\beta + \mathbf{u},$$

where $B = I_N \otimes \iota$, $\alpha = (\alpha_1, \ldots, \alpha_N)$, and $\otimes$ is the Kronecker product.

The MIDAS approach allows us to effectively reduce the dimensionality pertaining to the high-frequency lags. Alternatively, we may apply what is known as the UMIDAS scheme, see e.g., Foroni, Marcellino, and Schumacher (2015), and directly estimate the coefficients associated with each high-frequency covariate lags separately (see equation (8) in Section 5 for example). Such a strategy, which as Foroni, Marcellino, and Schumacher (2015) argue works in single regressions when the ratio high to low-frequency sampling is small, may not be appealing in high-dimensional cases, as the estimation and prediction performance deteriorates due to the potentially large number of coefficients; see Babii, Ghysels, and Striaukas (2022b) for further discussion.

While the theory we present is general, we have the specific empirical application of our paper in mind with a cross-section of firms for which we want to analyze corporate earnings predictions. Some firms belong to the same industry, or are of similar size, yet all are affected by the state of the macroeconomy as well. This calls for a panel regression setting where we exploit both the cross-sectional dimension and the time series dynamics.

Assuming that the individual lag coefficients in equation (1) are approximately sparse is *highly* restrictive. Instead, the approximate sparsity of slopes of the dictionary elements $(w_l)_{l\geq 0}$ is more plausible for many applications of interest to economists and will be maintained here as well.[3] For instance, if $w_0(s) = 1$ with $\beta_{0,k} \neq 0$ and $\beta_{l,k} = 0, \forall\ l \geq 1$, we recover the averaging of high-frequency lags of covariate k as a special case. More generally, the weight ω may be a decreasing function over lags and we may want to learn its shape from the data maximizing the predictive performance.[4]

[3]For a formal definition of approximate sparsity, see Babii, Ghysels, and Striaukas (2022b).

[4]See Ball and Easton (2013) and Ball and Gallo (2018) for further discussion on interpreting the shape of MIDAS polynomials in accounting data applications considered in our empirical application.

2.2 Fixed effect high-dimensional panel models

Given that the number of potential predictors K can be large, additional regularization can improve the predictive performance in small samples. To that end, we take advantage of the sg-LASSO regularization shown to be attractive for individual time series ML regressions in Babii, Ghysels, and Striaukas (2022b). The fixed effects panel data estimator with sparse-group regularization solves

$$\min_{(a,b)\in\mathbf{R}^{N+LK}} \|\mathbf{y} - Ba - \mathbf{X}b\|_{NT}^2 + 2\lambda\Omega(b), \tag{2}$$

where $\|.\|_{NT}^2 = |.|^2/(NT)$ is the empirical norm and

$$\Omega(b) = \gamma|b|_1 + (1-\gamma)\|b\|_{2,1}$$

is a regularizing functional, which is a linear combination of LASSO, i.e. $|b|_1$, and group LASSO penalties with for a group structure $\mathcal{G}$ described as a partition of $[p] = \{1, 2, \ldots, p\}$, the group LASSO norm is computed as $\|b\|_{2,1} = \sum_{G\in\mathcal{G}} |b_G|_2$. The parameter $\gamma \in [0,1]$ determines the relative weights of the ℓ_1 (sparsity) and the $\ell_{2,1}$ (group sparsity) norms, while the amount of regularization is controlled by the regularization parameter $\lambda \geq 0$. The group structure is assumed to be known to the econometrician, which in our setting corresponds to time series lags of covariates. For example, consider the earlier defined $T \times LK$ matrix of covariates $\mathbf{x}_i = (X_{i,1}W, \ldots, X_{i,K}W)$, where each $X_{i,1}W$ is a $T \times L$ matrix corresponding to the aggregated time series lags of predictor $k \in [K]$. Ignoring the fixed effects, the time series lags define a group structure with K groups of size L described as $\mathcal{G} = \{\{1, \ldots, L\}, \{L+1, \ldots, 2L\}, \ldots, \{p-L+1, \ldots, p\}\}$.

More generally, we may also combine covariates of a similar nature in groups. Throughout the paper we assume that groups have fixed size, which is well-justified in our empirical applications.[5] Therefore, the selection of covariates is performed by the group LASSO penalty, which encourages sparsity between groups. In addition, the ℓ_1 LASSO norm promotes sparsity within groups and allows us to learn the shape of the MIDAS weights from the data.

It is worth mentioning that the linear in parameters approximation to the MIDAS weight function leads to the convex optimization parameter problem in equation (2) that can be solved efficiently, e.g., via the proximal gradient descent algorithm, or its block-coordinate descent versions. In contrast, a popular beta weights leads to a nonlinear non-convex optimization problem that becomes challenging to solve in high-dimensions; cf. Marsilli (2014) and Khalaf, Kichian, Saunders, and Voia (2021).

[5] See Babii (2021) for a continuous-time mixed-frequency regression where the group size is allowed to increase with the sample size under the in-fill asymptotics.

3 Oracle inequalities

In this section, we provide the theoretical analysis of predictive performance of regularized panel data regressions with the sg-LASSO regularization, including the standard LASSO and the group LASSO regularizations as special cases. It is worth stressing that the analysis of this section is not tied to the mixed-frequency data setting and applies to the generic high-dimensional panel data regularized with the sg-LASSO penalty function. Importantly, we focus on panels consisting of potentially persistent τ-mixing time series with polynomial tails. Consider a generic panel data projection with a countable number of predictors

$$y_{i,t+h} = \alpha_i + \sum_{j=1}^{\infty} \beta_j x_{i,t,j} + u_{i,t}, \qquad \mathbb{E}[u_{i,t} x_{i,t,j}] = 0, \quad \forall j \geq 1,$$

This model subsumes the mixed-frequency data regressions as a special case, in which case covariates are obtained via a MIDAS weighting scheme with Legendre polynomials. The covariates may also include the time-varying covariates common for all entities (macroeconomic factors), lags of $y_{i,t}$, the intercept, as well as additional lags of a baseline covariate.

3.1 Dealing with temporal dependence: τ-mixing

Many empirical applications, such as the prediction of corporate earnings considered later in the paper, involve persistent time series data both as dependent variables and covariates. To that end, we follow Babii, Ghysels, and Striaukas (2022b) and measure the persistence of the data with τ-mixing coefficients. For a σ-algebra $\mathcal{M}$ and a random vector $\xi \in \mathbf{R}^l$, put

$$\tau(\mathcal{M}, \xi) = \left\| \sup_{f \in \text{Lip}_1} |\mathbb{E}(f(\xi)|\mathcal{M}) - \mathbb{E}(f(\xi))| \right\|_1,$$

where $\text{Lip}_1 = \{f : \mathbf{R}^l \to \mathbf{R} : \ |f(x) - f(y)| \leq |x - y|_1\}$ is a set of 1-Lipschitz functions from $\mathbf{R}^l$ to $\mathbf{R}$.[6] For a stochastic process $(\xi_t)_{t \in \mathbf{Z}}$ with a natural filtration generated by its past $\mathcal{M}_t = \sigma(\xi_t, \xi_{t-1}, \dots)$, the τ-mixing coefficients are defined as

$$\tau_k = \sup_{j \geq 1} \frac{1}{j} \sup_{t+k \leq t_1 < \cdots < t_j} \tau(\mathcal{M}_t, (\xi_{t_1}, \dots, \xi_{t_j})), \qquad k \geq 0 \tag{3}$$

[6] See Dedecker and Prieur (2004) and Dedecker and Prieur (2005) for equivalent definitions.

where the supremum is taken over all $t, t_1, \ldots, t_j \in \mathbf{Z}$. If $\tau_k \downarrow 0$, as $k \uparrow \infty$ then the process is called τ-mixing. The class of τ-mixing processes can be placed somewhere between the α-mixing processes and mixingales — the τ-mixing condition is less restrictive than the α-mixing condition, yet at the same time, there exists a convenient for us coupling result for τ-mixing processes, which is not the case for the mixingales or near-epoch dependent processes; see Dedecker and Doukhan (2003) and Dedecker and Prieur (2004, 2005) for more details.[7] This allows us to obtain concentration inequalities and performance guarantees for the sg-LASSO estimator; see Appendix B.

We would like to stress that the (non)asymptotic theory for the long panel data involves the concentration of double arrays

$$\sum_{i=1}^{N}\sum_{t=1}^{T}\xi_{i,t} = \sum_{i=1}^{N}\underbrace{\left(\sum_{t=1}^{T}\xi_{i,t}\right)}_{\equiv\xi_{i,T}} = \sum_{t=1}^{T}\underbrace{\left(\sum_{i=1}^{N}\xi_{i,t}\right)}_{\equiv\xi_{t,N}}$$

Instead of developing new results for such arrays, one could of course rely on the existing concentration inequalities for the i.i.d. or time-series data. However, this strategy does not lead to the optimal results for the heavy-tailed dependent data as it only reflects the concentration over one of the two dimensions — the i.i.d. inequality of Fuk and Nagaev (1971) applied to $\sum_{i=1}^{N}\xi_{i,T}$ does capture the benefits of the time dimension while the inequality of Babii, Ghysels, and Striaukas (2022a) applied to $\sum_{t=1}^{T}\xi_{t,N}$ does not capture the benefits of the cross-section. Our paper provides new Fuk-Nagaev and Rosenthal's inequalities for such double arrays consisting of τ-mixing processes as well as the central limit theorem when both the cross-section and the time dimension increase at the same time. Building on these results, we develop the inferential theory presented in subsequent sections.

3.2 Pooled regression

For pooled regressions, we assume that all entities share the same intercept parameter $\alpha_1 = \cdots = \alpha_N = \alpha$. The pooled sg-LASSO estimator $\hat{\rho} = (\hat{\alpha}, \hat{\beta}^\top)^\top$ solves

$$\min_{r=(a,b)\in\mathbf{R}^{1+p}} \|\mathbf{y} - a\iota - \mathbf{X}b\|_{NT}^2 + 2\lambda\Omega(r). \tag{4}$$

[7]The class of α-mixing processes is too restrictive for the predictive linear projection model with covariates and autoregressive lags; see also Babii, Ghysels, and Striaukas (2022b), Proposition A.3.1.

Define (a) $z_{i,t} = (1, x_{i,t}^\top)^\top$, where $x_{i,t} \in \mathbf{R}^p$ is a vector of predictors, (b) $u_i = (u_{i,1}, \ldots, u_{i,T})$ and (c) $x_i = (x_{i,1}^\top, \ldots, x_{i,T}^\top)^\top$ for $i \in [N]$. Let $\tau_k^{(i,j)}$ denote the τ-mixing coefficient of a stochastic process $(u_{i,t} z_{i,t,j})_{t \in \mathbf{Z}}$ with its natural filtration, where $i \in [N]$ and $j \in [p+1]$; see equation (3). Similarly, let $\tilde{\tau}_k^{(i,j)}$ denote the τ-mixing coefficient of j^{th} coordinate of $(\text{vech}(z_{i,t} z_{i,t}^\top))_{t \in \mathbf{Z}}$, where $i \in [N]$ and $j \in [(p+1)(p+2)/2]$. The following assumption imposes mild restrictions on the data.

Assumption 3.1 (Data)**.** $\{(u_i, x_i^\top)^\top : i \in \mathbf{N}\}$ *are independent vectors in* $\mathbf{R}^{(p+1)} \times \mathbf{R}^T$ *such that (i)* $\max_{i \in [N], t \in [T], j \in [p+1]} \|u_{i,t} z_{i,t,j}\|_q = O(1)$ *for some* $q > 2$*; (ii) the* τ*-mixing coefficients of* $(u_{i,t} z_{i,t})_{t \in \mathbf{Z}}$ *satisfy* $\max_{i \in [N], j \in [p+1]} \tau_{k-1}^{(i,j)} = O(k^{-a}), \forall k \geq 1$ *with* $a > (q-1)/(q-2)$*; (iii)* $\max_{i \in [N], t \in [T], j,k \in [p+1]} \|z_{i,t,j} z_{i,t,k}\|_{\tilde{q}} = O(1)$ *for some* $\tilde{q} > 2$*; (iv) the* τ*-mixing coefficients of* $\text{vech}((z_{i,t} z_{i,t}^\top))_{t \in \mathbf{Z}}$ *satisfy* $\max_{i \in [N], j \in [(p+1)(p+2)/2]} \tilde{\tau}_{k-1}^{(i,j)} \leq \tilde{c} k^{-\tilde{a}}, \forall k \geq 1$ *with* $\tilde{c} > 0$ *and* $\tilde{a} > (\tilde{q}-1)/(\tilde{q}-2)$*.*

Note that we do not impose stationarity over $t \in \mathbf{Z}$ and require that only $2 + \epsilon$ moments exist with $\epsilon > 0$, which is a realistic assumption in our empirical application and more generally for datasets encountered in time series and financial econometrics applications. Note also that the time series dependence is assumed to fade away relatively slowly — at a polynomial rate as measured by the τ-mixing coefficients.

Next, we assume that the $(1+p) \times (1+p)$ matrix $\Sigma_{N,T} = \frac{1}{NT} \sum_{i=1}^N \sum_{t=1}^T \mathbb{E}[z_{i,t} z_{i,t}^\top]$ exists and is non-singular uniformly over N, T, p:

Assumption 3.2 (Covariance matrix)**.** *The smallest eigenvalue of* $\Sigma_{N,T}$ *is uniformly bounded away from zero by some universal constant* $\gamma_{\min} > 0$*.*

Assumption 3.2 is satisfied for the spiked identity and Topelitz covariance structures. It can be interpreted as a completeness condition, see Babii and Florens (2020), and can also be relaxed to the restricted eigenvalue condition imposed on the population covariance matrix $\Sigma_{N,T}$; see Babii, Ghysels, and Striaukas (2022b). We can also allow for $\gamma_{\min} \downarrow 0$ as $N, T, p \uparrow \infty$, in which case $\gamma_{\min}^{-1}$ would slow down the convergence rates in oracle inequalities and could be interpreted as a measure of ill-posedness; see also Carrasco, Florens, and Renault (2007).

Lastly, we assume that the regularization parameter λ scales appropriately with the number of covariates p, the length of the panel T, the size of the cross-section N, and a certain exponent κ that depends on the tail parameter q and the persistence parameter a. The precise order of the regularization parameter is described by the Fuk-Nagaev inequality for long panels appearing in the Appendix; see Theorem A.1.

Assumption 3.3 (Regularization). *For some* $\delta \in (0,1)$

$$\lambda \sim \left(\frac{p}{\delta(NT)^{\kappa-1}}\right)^{1/\kappa} \vee \sqrt{\frac{\log(p/\delta)}{NT}},$$

where $\kappa = ((a+1)q-1)/(a+q-1)$ *and* a, q *are as in Assumptions 3.1.*

Our first result is the oracle inequality for the pooled sg-LASSO estimator described in equation (4). The result allows for misspecified regressions with a non-trivial approximation error in the sense that we consider more generally

$$\mathbf{y} = \mathbf{m} + \mathbf{u},$$

where $\mathbf{m} \in \mathbf{R}^{NT}$ is approximated with $\mathbf{Z}\rho$, $\mathbf{Z} = (\iota, \mathbf{X})$, $\iota \in \mathbf{R}^{NT}$ is all-ones vector, and $\rho = (\alpha, \beta^\top)^\top$. The approximation error $\mathbf{m} - \mathbf{Z}\rho$ might come from the fact that the MIDAS weight function may not have the exact expansion in terms of the specified dictionary or from the fact that some of the relevant predictors are not included in the regression equation. To state the result, let $S_0 = \{j \in [p] : \beta_j \neq 0\}$ be the support of β and let $\mathcal{G}_0 = \{G \in \mathcal{G} : \beta_G \neq 0\}$ be the group support of β. Consider the *effective sparsity* of the sparse-group structure, defined as $s^{1/2} = \gamma\sqrt{|S_0|} + (1-\gamma)\sqrt{|\mathcal{G}_0|}$. Note that s is proportional to the sparsity $|S_0|$, when $\gamma = 1$ and to the group sparsity $|\mathcal{G}_0|$ when $\gamma = 0$. Define $r_{N,T}^{\text{pooled}} = s^{\tilde{\kappa}}p^2/(NT)^{\tilde{\kappa}-1} + p^2\exp(-cNT/s^2)$.

Theorem 3.1. *Suppose that Assumptions 3.1, 3.2, and 3.3 are satisfied. Then with probability at least* $1 - \delta - O(r_{N,T}^{\text{pooled}})$

$$\|\mathbf{Z}(\hat{\rho} - \rho)\|_{NT}^2 \lesssim s\lambda^2 + \|\mathbf{m} - \mathbf{Z}\rho\|_{NT}^2$$

and

$$|\hat{\rho} - \rho|_1 \lesssim s\lambda + \lambda^{-1}\|\mathbf{m} - \mathbf{Z}\rho\|_{NT}^2 + s^{1/2}\|\mathbf{m} - \mathbf{Z}\rho\|_{NT},$$

for some $c > 0$ *and* $\tilde{\kappa} = ((\tilde{a}+1)\tilde{q}-1)/(\tilde{a}+\tilde{q}-1)$.

The proof of this result can be found in the Appendix. Theorem 3.1 describes the non-asymptotic oracle inequalities for the prediction and the estimation accuracy in the environment where the number of regressors p is allowed to scale with the effective sample size NT. Importantly, the result is stated under the weak tail and persistence conditions in Assumption 3.1. Parameters κ and $\tilde{\kappa}$ are the dependence-tails exponents for stochastic processes driving the regression score and the covariance matrix respectively. Theorem 3.1 shows that the prediction and the estimation accuracy of pooled panel data regressions improves when the sparse-group structure is taken

into account. Indeed, for the LASSO regression, the effective sparsity reduces to $s^{1/2} = \sqrt{|S_0|}$, which is larger than $\gamma\sqrt{|S_0|} + (1-\gamma)\sqrt{|\mathcal{G}_0|}$ in the case of sg-LASSO.

The proof of Theorem 3.1 relies on the developments in Babii, Ghysels, and Striaukas (2022b) with some improvements. Notably, it relies on the new Fuk-Nagaev concentration inequality for long panel data, see Theorem A.1.

Next, we consider the convergence rates of the prediction and estimation errors. The following assumption considers a simplified setting, where the approximation error vanishes sufficiently fast, and the total number of regressors vanishes sufficiently fast with the effective sample size NT.

Assumption 3.4. *(i)* $\|\mathbf{m} - \mathbf{Z}\rho\|_{NT}^2 = O_P(s\lambda^2)$*; and (ii)* $s^{\tilde{\kappa}}p^2(NT)^{1-\tilde{\kappa}} \to 0$ *and* $p^2\exp(-cNT/s^2) \to 0$*.*

Note that Assumption 3.4 allows for (1) $N \to \infty$ while T is fixed; (2) $T \to \infty$ while N is fixed; and (3) both $N \to \infty$ and $T \to \infty$ without restricting the relative growth of the two. The following result describes the prediction and the estimation convergence rates in the asymptotic environment outlined in Assumption 3.4 and is an immediate consequence of Theorem 3.1.

Corollary 3.1. *Suppose that Assumptions 3.1, 3.2, 3.3, and 3.4 are satisfied. Then*

$$\|\mathbf{Z}(\hat{\rho} - \rho)\|_{NT}^2 = O_P\left(\frac{sp^{2/\kappa}}{(NT)^{2-2/\kappa}} \vee \frac{s\log p}{NT}\right)$$

and

$$|\hat{\rho} - \rho|_1 = O_P\left(\frac{sp^{1/\kappa}}{(NT)^{1-1/\kappa}} \vee s\sqrt{\frac{\log p}{NT}}\right).$$

Corollary 3.1 describes the prediction and the estimation accuracy of pooled sparse-group panel data regressions. It suggests that the predictive performance of the sg-LASSO (and consequently LASSO and group LASSO) regressions may deteriorate when regression errors and/or predictors are heavy-tailed or when the data are extremely persistent. However, for geometrically ergodic Markov processes, e.g., stationary AR(1) process, the τ-mixing coefficients decline geometrically fast, so that $\kappa \approx q$ and $\tilde{\kappa} \approx \tilde{q}$. In this case, the prediction accuracy scales approximately at the rate $O_P\left(\frac{p^{2/q}}{(NT)^{2-2/q}} \vee \frac{\log p}{NT}\right)$ and the predictive performance may be affected only by the tails constant q.

If additionally the data are sub-Gaussian, then moments of all order $q \geq 2$ exist, and for any particular effective sample size NT, the first term can be made arbitrarily

small relatively to the second term. In this case we recover the $O_P(\log p/NT)$ rate typically obtained for sub-Gaussian data. On the other hand, if the polynomial tail dominates, then we need $p = o((NT)^{q-1})$ for the prediction and the estimation consistency provided that $\tilde{q} \geq 2q-1$ and the sparsity constant s is fixed. In this case, we have a *significantly weaker* requirement than the $p = o(T^{q-1})$ condition needed for time series regressions in Babii, Ghysels, and Striaukas (2022b). Moreover, since $q > 2$, $p = o((NT)^{q-1})$ can be significantly weaker than the $p = o(NT)$ condition typically needed for QMLE/GMM estimators without regularization.

Theorem 3.1 and Corollary 3.1 imply two practical consequences: (1) one may want to exclude (or suitably transform) the heavy-tailed series from the predictive regressions based on the preliminary estimates of the tail index, e.g., using the Hill estimator; (2) if the individual heterogeneity can be ignored, then pooling panel data can improve significantly the predictive performance. In the latter case, one can also cluster similar series in groups, e.g., based on the unsupervised clustering algorithms, which may strike a good balance between the pooling benefits and heterogeneity.

3.3 Fixed effects

Pooled regressions are attractive since the effective sample size NT can be huge, yet the heterogeneity of individual time series may be lost. If the underlying series have a substantial heterogeneity over $i \in [N]$, then taking this into account might reduce the projection error and improve the predictive accuracy. At a very extreme side, the cross-sectional structure can be completely ignored and individual time series regressions can be used for prediction. The fixed effects panel data regressions strike a good balance between the two extremes controlling for heterogeneity with entity-specific intercepts.

The fixed effects sg-LASSO estimator $\hat{\rho} = (\hat{\alpha}^\top, \hat{\beta}^\top)^\top$ solves

$$\min_{(a,b)\in\mathbf{R}^{N+p}} \|\mathbf{y} - Ba - \mathbf{X}b\|_{NT}^2 + 2\lambda\Omega(b),$$

where $B = I_N \otimes \iota$, I_N is $N \times N$ identity matrix, $\iota \in \mathbf{R}^T$ is an all-ones vector, and Ω is the sg-LASSO regularizing functional. It is worth stressing that the design matrix $\mathbf{X}$ does not include the intercept and that we do not penalize the fixed effects, that are typically not sparse. By Fermat's rule, the first-order conditions are

$$\begin{aligned} \hat{\alpha} &= (B^\top B)^{-1} B^\top (\mathbf{y} - \mathbf{X}\hat{\beta}) \\ 0 &= \mathbf{X}^\top M_B (\mathbf{X}\hat{\beta} - \mathbf{y})/NT + \lambda z^* \end{aligned} \tag{5}$$

for some $z^* \in \partial\Omega(\hat{\beta})$, where $b \mapsto \partial\Omega(b)$ is the subdifferential of Ω and $M_B = I - B(B^\top B)^{-1}B^\top$ is the orthogonal projection matrix. It is easy to see from the first-order conditions that the estimator of $\hat{\beta}$ is equivalent to 1) penalized GLS estimator for the first-differenced regression; 2) penalized OLS estimator for the regression written in the deviation from time means; and 3) penalized OLS estimator where the fixed effects are partialled-out. Therefore, the equivalence between the three approaches is not affected by the penalization; cf. Arellano (2003) for low-dimensional panels.

With some abuse of notation, redefine

$$\hat{\Sigma}_{N,T} = \begin{pmatrix} \frac{1}{T}B^\top B & \frac{1}{\sqrt{NT}}B^\top \mathbf{X} \\ \frac{1}{\sqrt{NT}}\mathbf{X}^\top B & \frac{1}{NT}\mathbf{X}^\top \mathbf{X} \end{pmatrix} \quad \text{and} \quad \Sigma_{N,T} = \begin{pmatrix} I_N & \frac{1}{\sqrt{NT}}\mathbb{E}\left[B^\top \mathbf{X}\right] \\ \frac{1}{\sqrt{NT}}\mathbb{E}\left[\mathbf{X}^\top B\right] & \mathbb{E}[x_{i,t}x_{i,t}^\top] \end{pmatrix}. \tag{6}$$

In line with Assumption 3.2 we will assume that the smallest eigenvalue of $\Sigma_{N,T}$ is uniformly bounded away from zero by some constant. Note that if $x_{i,t} \sim N(0, I_p)$, then $\Sigma_{N,T} = I_{N+p}$ and this assumption is trivially satisfied.

Next, we make an assumption about the order of the regularization parameter which is governed by the Fuk-Nagaev inequality for long panels; see Appendix, Theorem A.1.

Assumption 3.5 (Regularization)**.** *For some* $\delta \in (0, 1)$

$$\lambda \sim \left(\frac{p \vee N^{\kappa/2}}{\delta(NT)^{\kappa-1}}\right)^{1/\kappa} \vee \sqrt{\frac{\log(p \vee N/\delta)}{NT}},$$

where $\kappa = ((a+1)q - 1)/(a + q - 1)$*, and* a, q *are as in Assumptions 3.1.*

Similarly to the pooled regressions, we state the oracle inequality allowing for the approximation error. For fixed effects regressions, with some abuse of notation we redefine $\mathbf{Z} = (B, \mathbf{X})$ and $\rho = (\alpha^\top, \beta^\top)^\top$. Put also $r^{\text{fe}}_{N,T} = p(s \vee N)^{\tilde{\kappa}}T^{1-\tilde{\kappa}}(N^{1-\tilde{\kappa}/2} + pN^{1-\tilde{\kappa}}) + p(p \vee N)e^{-cNT/(s\vee N)^2}$ with $\tilde{\kappa} = ((\tilde{a}+1)\tilde{q} - 1)/(\tilde{a} + \tilde{q} - 1)$ and some $c > 0$.

Theorem 3.2. *Suppose that Assumptions 3.1, 3.2, and 3.5 are satisfied. Then with probability at least* $1 - \delta - O(r^{\text{fe}}_{N,T})$

$$\|\mathbf{Z}(\hat{\rho} - \rho)\|^2_{NT} \lesssim (s \vee N)\lambda^2 + \|\mathbf{m} - \mathbf{Z}\rho\|^2_{NT}.$$

Theorem 3.2 states a non-asymptotic oracle inequality for the prediction error in the fixed effects panel data regressions estimated with the sg-LASSO. To see clearly, how the prediction accuracy scales with the sample size, we make the following assumption.

Assumption 3.6. *Suppose that (i)* $\|\mathbf{m}-\mathbf{Z}\rho\|_{NT}^2 = O_P((s\vee N)\lambda^2)$*; (ii)* $(p+N^{\tilde{\kappa}/2})p(s\vee N)^{\tilde{\kappa}}N^{1-\tilde{\kappa}}T^{1-\tilde{\kappa}} \to 0$ *and* $p(p\vee N)e^{-cNT/(s\vee N)^2} \to 0$.

Then the following corollary is an immediate consequence of Theorem 3.2.

Corollary 3.2. *Suppose that Assumptions 3.1, 3.2, 3.5, and 3.6 are satisfied. Then*

$$\|\mathbf{Z}(\hat{\rho}-\rho)\|_{NT}^2 = O_P\left(\frac{(s\vee N)(p^{2/\kappa}\vee N)}{N^{1-2/\kappa}T^{2-2/\kappa}} \vee \frac{(s\vee N)\log(p\vee N)}{NT}\right).$$

Corollary 3.2 allows for $s, p, N, T \to \infty$ at appropriate rates. However, we pay an additional price for estimating N fixed effects which plays a role similar to the effective dimension of covariates. An immediate practical implication is that to achieve accurate predictions with high-dimensional fixed effect regressions, the panel has to be sufficiently long to offset the estimation error of the individual fixed effects. Likewise, the tails and the persistence of the data may also reduce the prediction accuracy in small samples through κ, which is approximately equal to q for geometrically decaying τ-mixing coefficients.

4 Debiased inference

In many empirical applications we are not only interested in building machine learning empirical panel data prediction models. We often also want to test hypotheses of interest as is the case in our empirical application where we want to identify the covariates which are significant in explaining prediction errors in a panel of analyst earnings predictions.

In this section, we therefore develop the debiased inferential methods for pooled panel data regressions. For a vector $\rho \in \mathbf{R}^{p+1}$, we use $\rho_G \in \mathbf{R}^{|G|}$ to denote the subvector of elements of $\rho \in \mathbf{R}^{p+1}$ indexed by $G \subset [p+1]$. Let $B = \hat{\Theta}\mathbf{Z}^\top(\mathbf{y}-\mathbf{Z}\hat{\rho})/NT$ denote the bias-correction for the sg-LASSO estimator, where $\hat{\Theta}$ is the nodewise LASSO estimator of the precision matrix $\Theta = \Sigma^{-1}$, where $\Sigma = \mathbb{E}[z_{i,t}z_{i,t}^\top]$. For pooled panel data, this estimator can be obtained as follows:

1. For each $j \in [p+1]$, let $\hat{\mu}_j = (\hat{\mu}_{j,1}, \ldots, \hat{\mu}_{j,p})^\top$ be a solution to

$$\min_{\mu\in\mathbf{R}^p} \|\mathbf{Z}_j - \mathbf{Z}_{-j}\mu\|_{NT}^2 + 2\lambda_j|\mu|_1,$$

where $\mathbf{Z}_j$ is $NT \times 1$ vector of stacked observations $\{z_{i,t,j} \in \mathbf{R} : i \in [N], t \in [T]\}$ and $\mathbf{Z}_{-j}$ is the $NT \times p$ matrix of stacked observations $\{(z_{i,t,k})_{k\neq j} \in \mathbf{R}^p : i \in [N], t \in [T]\}$. Put

$$\hat{\sigma}_j^2 = \|\mathbf{Z}_j - \mathbf{Z}_{-j}\hat{\mu}_j\|_{NT}^2 + \lambda_j|\hat{\mu}_j|,$$

2. Compute $\hat{\Theta} = \hat{B}^{-1}\hat{C}$, where $\hat{B} = \text{diag}(\hat{\sigma}_1^2, \ldots, \hat{\sigma}_{p+1}^2)$, and

$$\hat{C} = \begin{pmatrix} 1 & -\hat{\mu}_{1,1} & \ldots & -\hat{\mu}_{1,p} \\ -\hat{\mu}_{2,1} & 1 & \ldots & -\hat{\mu}_{2,p} \\ \vdots & \vdots & \ddots & \vdots \\ -\hat{\mu}_{p,1} & \ldots & -\hat{\mu}_{p,p} & 1 \end{pmatrix}.$$

Let $v_{i,t,j} = z_{i,t,j} - \sum_{k \neq j} \mu_{j,k} z_{i,t,k}$ be the regression error for j^{th} nodewise LASSO regression. Let s_j be the number of non-zero elements in j^{th} row of precision matrix Θ_j, and put $S = \max_{j \in G} s_j$, and $s^* = s \vee S$.

The following assumption describes an additional set of conditions for the debiased central limit theorem.

Assumption 4.1. *(i)* $\sup_z \mathbb{E}[u_{i,t}^2 | z_{i,t} = z] = O(1)$*; (ii)* $\|\Theta_G\|_\infty = O(1)$ *for* $G \subset [p+1]$ *of fixed size; (iii) the long run variance of* $(u_{i,t}^2)_{t \in \mathbf{Z}}$ *and* $(v_{i,t,j}^2)_{t \in \mathbf{Z}}$ *exists for every* $j \in G$*; (iv)* $s^{*2} \log^2 p / T \to 0$ *and* $p / \sqrt{T^{\kappa-2} \log^\kappa p} \to 0$*; (v)* $\|\mathbf{m} - \mathbf{Z}\rho\|_{NT} = o_P(1/\sqrt{NT})$*; (vi) for every* $j, l \in [p]$ *and* $k \geq 0$*, the* τ*-mixing coefficients of* $(u_{i,t} u_{i,t+k} x_{i,t,j} x_{i,t+k,l})_{t \in \mathbf{Z}}$ *are* $\check{\tau}_t \leq c t^{-d}$ *for some universal constants* $c > 0$ *and* $d > 1$*; (vi) for each* i*,* $\{(u_{i,t}, z_{i,t}^\top)^\top : t \in \mathbf{Z}\}$ *is a stationary process that is also i.i.d. over* i*, Assumption 3.1 holds with* $a > (q-1)/(q-2) \vee (q\delta + 1)/(q - 2 - \delta)$ *with* $q > 2 + \delta$ *and* $\delta > 0$*.*

Assumption 4.1 (i) requires that the conditional variance of the regression error is bounded. Condition (ii) requires that the rows of the precision matrix have bounded ℓ_1 norm and is a plausible assumption in the high-dimensional setting, where the inverse covariance matrix is often sparse. Condition (iii) is a mild restriction needed for the consistency of the sample variance of regression errors. The rate conditions in (iv) are similar to the condition used in Babii, Ghysels, and Striaukas (2022a). Lastly, condition (v) is trivially satisfied when the projection coefficients are sparse and, more generally, it requires that the misspecification error vanishes asymptotically sufficiently fast.

The following result describes a large-sample approximation to the distribution of the debiased sg-LASSO estimator with serially correlated heavy-tailed errors.

Theorem 4.1. *Suppose that Assumptions 3.1, 3.2, 3.3, 3.4, and 4.1 are satisfied for the sg-LASSO regression and for each nodewise LASSO regression* $j \in G$*. Then*

$$\sqrt{NT}(\hat{\rho}_G + B_G - \rho_G) \xrightarrow{d} N(0, \Xi_G)$$

with the long-run variance $\Xi_G = \lim_{T \to \infty} \text{Var}\left(\frac{1}{\sqrt{T}} \sum_{t=1}^T u_{i,t} \Theta_G z_{i,t}\right)$.

Theorem 4.1 applies to panel data consisting of non-Gaussian, heavy-tailed, and persistent time series under the large N and T large sample approximation. In contrast to the fixed T approximations, Theorem 4.1 leads to more precise inference, e.g., the standard errors and the length of confidence intervals would scale at $O(1/\sqrt{NT})$ rate instead of $O(1/\sqrt{N})$ that we typically encounter for fixed T approximations or $O(1/\sqrt{T})$ for individual time series regressions considered in Babii, Ghysels, and Striaukas (2022b). Note that this result is used in our empirical application to perform the Granger causality test based on the following Wald statistic

$$W_{NT} = NT(\hat{\rho}_G + B_G - \rho_G)\hat{\Xi}_G^{-1}(\hat{\rho}_G + B_G - \rho_G) \xrightarrow{d} \chi^2_{|G|}.$$

To estimate Ξ_G, we can use the following pooled HAC estimator

$$\hat{\Xi}_G = \frac{1}{N}\sum_{i=1}^{N}\sum_{|k|<T} K\left(\frac{k}{M_T}\right)\hat{\Gamma}_{k,i},$$

where $\hat{\Gamma}_{k,i} = \hat{\Theta}_G\left(\frac{1}{T}\sum_{t=1}^{T-k}\hat{u}_{i,t}\hat{u}_{i,t+k}x_{i,t}x_{i,t+k}^\top\right)\hat{\Theta}_G^\top$, $\hat{u}_{i,t}$ is the sg-LASSO residual, and $\hat{\Gamma}_{-k,i} = \hat{\Gamma}_{k,i}^\top$. The kernel function $K : \mathbf{R} \to [-1,1]$ with $K(0) = 1$ is puts less weight on more distant noisy covariances, while $M_T \uparrow \infty$ is a bandwidth (or lag truncation) parameter; see Babii, Ghysels, and Striaukas (2022a) for more details as well as formal results on the validity of HAC-based inference using sg-LASSO residuals.

5 Monte Carlo simulations

In this section, we assess the finite sample performance of the Granger causality tests for high-dimensional pooled panel data MIDAS regressions. A first subsection describes the design, followed by a second reporting the findings.

5.1 Design

We simulate the data from the following DGP:

$$y_{i,t} = \alpha + \rho y_{i,t-1} + \sum_{k=1}^{K}\frac{1}{m}\sum_{j=1}^{m}\omega((j-1)/m;\beta_k)x_{i,t-(j-1)/m,k} + u_{i,t}, \tag{7}$$

where $i \in [N]$, $t \in [T]$, α is the the common intercept, $\frac{1}{m}\sum_{j=1}^{m}\omega((j-1)/m;\beta_k)$ is the weight function for k-th high-frequency covariate and the error term is $u_{i,t} \sim_{i.i.d.}$

$N(0,4)$. The DGP corresponds to the target variable of interest $y_{i,t}$ driven by one autoregressive lag augmented with high-frequency series. The DGP is therefore a pooled MIDAS panel data model.

We set $\rho = 0.15$ and take the first high-frequency regressor, $k = 1$, as relevant, i.e. the first regressor Granger causes the response variable. We are interested in quarterly/monthly data, and use four quarters of data for the high-frequency regressors so that $m = 12$. The high-frequency regressors are generated as K i.i.d. realizations of univariate autoregressive (AR) processes $x_h = \rho x_{h-1} + \varepsilon_h$, where $\rho = 0.7$ and $\varepsilon_h \sim_{i.i.d.} N(0,1)$, where h denotes the high-frequency sampling. For the DGP we rely on a commonly used weighting scheme in the MIDAS literature, namely the weights $\omega(s;\beta_k)$ for the only relevant high-frequency regressor $k = 1$ determined by the beta density, Beta$(3,3)$; see Ghysels, Sinko, and Valkanov (2007) or Ghysels and Qian (2019), for further details. The empirical estimation involves MIDAS regressions with Legendre polynomials of degree $L = 3$. Lastly, we draw the intercepts $\alpha \sim$ Uniform$(-4,4)$. Throughout the experiment, we fix the sample sizes to $T = 50$ and $N = 30$.

We compare the empirical size and power of the Granger causality test under different structures placed on the regression models.

First, we compare sg-LASSO-MIDAS with LASSO-UMIDAS pooled panel data models. The former exploits the group structure of covariates by applying the sg-LASSO penalty function and a flexible way to model lags for each covariate using the MIDAS weight functions parametrized by low-dimensional coefficients. The latter pertains to the unstructured LASSO estimator together with the UMIDAS scheme. Introduced by Foroni, Marcellino, and Schumacher (2015), UMIDAS consists of estimating a regression coefficient for each high-frequency lag separately, and therefore the weight function for each covariate is

$$\sum_{j=1}^{m} \omega((j-1)/m;\beta_k) x_{i,t-(j-1)/m,k} = \sum_{j=1}^{m} b_{j,k} x_{i,t-(j-1)/m,k} \tag{8}$$

where $b_{j,k}$ is a regression coefficient associated with each high-frequency lag. We estimate regression coefficients by applying the standard unstructured LASSO estimator; hence we call the model LASSO-UMIDAS.

Second, we compare the pooled panel with individual time series regressions, for sg-LASSO-MIDAS and LASSO-UMIDAS, where the former exploits the benefits of the panel structure and the latter does not. In this case, we take the first sample $i = 1$ to compute empirical size and power of the Granger test for the individual

regression models. Babii, Ghysels, and Striaukas (2022a) propose tests of Granger causality in univariate regularized regressions and high-dimensional data.

Pooled Panel

	Parzen kernel				*Quadratic spectral kernel*			
$M_T \backslash a$	0	1/5	1/4	1/3	0	1/5	1/4	1/3
				sg-LASSO-MIDAS				
10	0.051	0.835	0.959	0.999	0.056	0.841	0.963	0.998
20	0.049	0.822	0.954	0.999	0.047	0.828	0.957	0.998
30	0.046	0.803	0.953	0.999	0.047	0.823	0.956	0.998
				LASSO-UMIDAS				
10	0.039	0.551	0.788	0.978	0.042	0.549	0.797	0.979
20	0.030	0.514	0.762	0.970	0.033	0.535	0.780	0.977
30	0.021	0.494	0.735	0.964	0.025	0.514	0.758	0.972

Individual Regressions

	Parzen kernel				*Quadratic spectral kernel*			
$M_T \backslash a$	0	1/5	1/4	1/3	0	1/5	1/4	1/3
				sg-LASSO-MIDAS				
10	0.090	0.356	0.406	0.548	0.094	0.349	0.356	0.486
20	0.097	0.345	0.406	0.548	0.094	0.350	0.360	0.492
30	0.092	0.345	0.403	0.547	0.093	0.356	0.379	0.524
				LASSO UMIDAS				
10	0.110	0.201	0.228	0.362	0.107	0.210	0.236	0.378
20	0.111	0.240	0.272	0.406	0.108	0.212	0.206	0.388
30	0.107	0.245	0.370	0.494	0.105	0.204	0.206	0.386

Table 1: HAC-based inference simulation results — We report results for a set of bandwidth parameters, denoted M_T, and two kernel functions.

5.2 Simulation results

In Table 1, we report the empirical rejection frequency (ERF) for the Granger causality test based on the HAC estimator with two different kernel functions, Parzen and Quadratic spectral, and two different estimation strategies, sg-LASSO-MIDAS and LASSO-UMIDAS. We test whether the first high-frequency covariate Granger causes the low-frequency series, which corresponds to the DGP potential causal pattern. We report results for a set of bandwidth parameters, denoted $M_T = 10$, 20 and 30. The reported results are based on 2000 Monte Carlo replications.

To assess the performance we scale the Beta density function by multiplying it with a constant $a \in \{0, 1/5, 1/4, 1/3\}$, i.e. the weight function for the relevant covariate is:

$$a\frac{1}{m}\sum_{j=1}^{m}\omega((j-1)/m;\beta_k)$$

For $a = 0$, the ERF shows the empirical size of the test for the nominal level of 5%, while $a \in \{1/5, 1/4, 1/3\}$ the ERF shows the empirical power of the Granger causality test. For the larger scaling constant a, the alternatives are separated further away from the null hypothesis and the Granger causality test is expected to perform better.

The results reported in Table 1 show that the Granger causality test based on the sg-LASSO-MIDAS has empirical size close to the nominal level of 5%. In contrast, the LASSO-UMIDAS leads to undersized Granger causality tests with size distortions around 0.01. The Granger causality test based on the sg-LASSO-MIDAS has also better empirical power against each of the alternative hypotheses $a \in \{1/5, 1/4, 1/3\}$. Additionally, it approaches 1 much faster as opposed to the LASSO-UMIDAS.

The results for individual regressions reveal worse performance compared to pooled panel data regressions, hence showing the usefulness of pooling the data. The empirical size shows considerable size distortions of around 0.05. Tests for individual regressions have worse power compared to the pooled panel data cases. Nonetheless, similar to the pooled panel data cases, the sg-LASSO-MIDAS estimation method seems to have better empirical power when comparing to LASSO-UMIDAS.

Overall, the results of the Monte Carlo experiments indicate that the structured regularization leads to better Granger causality tests in small samples.

6 Do analysts leave money on the table?

In this section we revisit a topic raised by Ball and Ghysels (2018) and Carabias (2018). Their empirical findings suggest that analysts tend to focus on their firm/industry when making earnings predictions while not fully taking into account the impact of macroeconomic events. While their findings were suggestive, there was no formal testing in a data-rich environment. The theory established in the previous sections allows us to do so.

More specifically, we consider the earnings of 210 US firms using a set of predictors sampled at mixed frequencies — quarterly, monthly and daily series. We use 26 predictors (and their lags), including traditional macro and financial series as well as non-standard series generated by textual analysis of financial news.

6.1 Data description

The full sample consists of observations between the 1^{st} of January, 2000 and the 30^{th} of June, 2017. Due to the lagged dependent variables in the models, our effective

sample starts at the third fiscal quarter of 2000. We collected data from CRSP and I/B/E/S to compute quarterly earnings and firm-specific financial covariates; RavenPack was used to compute daily firm-level textual-analysis-based data; real-time monthly macroeconomic series are from the ALFRED; FRED is used to compute daily financial markets data and, lastly, monthly news attention series extracted from the *Wall Street Journal* articles were retrieved from Bybee, Kelly, Manela, and Xiu (2019).[8] Table 2 provides a list of the variables used in our analysis, whereas Online Appendix Section OA.1 covers a detailed description of the RavenPack data. Finally, the list of all firms we consider in our analysis appears in Online Appendix Table OA.1. Table 2 has six panels, namely three panels of firm-level series: A1 – describes earnings data, B1 – describes daily firm-level stock market data, and C1 – describes daily firm-level sentiment data series. The remaining three panels are: A2 – describes real-time monthly macro series, B2 – describes daily financial markets data, and C2 – describes monthly news attention series. In the models we include 365 daily lags, 12 monthly lags and 4 quarterly lags respectively.

6.2 Granger causality tests

Whether analysts leave money on the table amounts to testing whether forecast errors in earnings can be predicted by current information variables. Hence, this amounts to performing something akin to the Granger causality test. In our empirical application we are dealing with a panel, and it is important to exploit the multivariate data structure to perform such tests.

We analyze the difference between realized earnings and analysts' predictions, i.e., the response variable $y_{i,t+1}$ is computed by taking the difference between realized earnings, denoted $e_{i,t+1}$, and the median of analysts' predictions for the quarter $t+1$, denoted $f_{i,t+1|t}$,

$$y_{i,t+1} = e_{i,t+1} - f_{i,t+1|t}.$$

We then fit the following pooled panel data MIDAS model using sg-LASSO estimator:

$$y_{i,t+1} = \alpha + \rho y_{i,t} + \sum_{k=1}^{K} \psi(L^{1/m}; \beta_k) x_{i,t,k} + u_{i,t+1}. \tag{9}$$

We test which factors Granger cause future errors of earnings forecasts made by the analysts. In the sg-LASSO, groups are defined as all lags of a single covariate k; Legendre polynomials up to degree three are applied to all weight functions $\psi(L^{1/m}; \beta_k)$.

[8]The dataset is publicly available at http://www.structureofnews.com/.

We use 5-fold cross-validation to tune both λ and γ, where we define folds as adjacent blocks over the time series dimension to take into account the time series dependence. Similarly, we estimate the precision matrix using nodewise LASSO regressions selecting the tuning parameter in a similar vein. The results are reported in Table 3.

In Panel (A) of Table 3 we find that the AR(1) lag is significant, leading us to conclude that the prediction errors made by the analysts are persistent. The autoregressive coefficient is significant throughout all specifications of the models, including in a simple pooled AR(1) model. In the latter case, the AR(1) coefficient is estimated to be 0.147.

Panel (B) of Table 3 reports that beyond the AR(1) we find that the highly significant covariates are TED rate, CPI inflation and real GDP growth. These results support previous findings that analysts tend to miss information associated with macroeconomic conditions — including real GDP growth and the TED spread, which is an indicator of measure credit risk. The latter is rather surprising, as it indicates that analysts tend to miss out on credit risk information at the macro level in their earnings forecasts. Lastly, the term spread (10-year less 3-month treasury yield), often viewed as a business cycle indicator, is also significant at the 10% level.

Finally, in Panel (C) of Table 3 we report results based on the unstructured LASSO applying UMIDAS for the lag polynomials of each covariate. The findings reveal similar results for the TED rate, but notably miss real GDP and CPI inflation as significant covariates.

In Table 4 we show results based on a different way of pooling analysts' prediction errors $y_{i,t+1}$. We split the data into two parts based on how large the average disagreement among analysts is. For each firm, we compute the forecast disagreement as the difference between 95% and 5% percentile of the empirical forecast distribution and take the average over the sample. We sort from high to low disagreement and split the sample of firms into two subsamples of equal size. The results show that macro variables which are significant for the full sample are also significant for the large disagreement subsample. On the other hand, little significance is reported for the low disagreement subsample. In this case, only the AR(1) lag and stock returns are significant at the 5% significance level.

Lastly, in Figure 1 we plot the ratio of firms for which we find Granger causality based on individual regressions versus panel models. In Panel (a) we plot the ratios for sg-LASSO estimator using MIDAS weighting scheme while in Panel (b) we plot the ratios for the LASSO estimator with UMIDAS scheme. The plot shows ratios for each covariate representing the fraction with respect to sg-LASSO (Panel (a)) or

LASSO with UMIDAS (Panel (b)) each covariate is significant by running individual regressions. For example, the AR(1) lag is significant for around 30% (0.3) of firms when running individual sg-LASSO-MIDAS regressions. Some covariates that are not significant in pooled panels are significant for some firms; therefore, we show results for all covariates, including those that are not significant in pooled panel cases. We also show how the ratios differ for low (dark-gray color) versus high disagreement (light-gray color) firms. They represent whether a specific firm we run an individual regression for is in the high-disagreement versus low-disagreement subsample. Interestingly, the largest ratios are for AR(1), TED rate, Real GDP, CPI inflation and term spread in the case of sg-LASSO-MIDAS. Moreover, the portion of firms in the high disagreement subsample seem to have the largest ratios. In the case of LASSO-UMIDAS, the ratios show a less clear pattern, with only the AR(1) and TED rate covariates significant for a larger number of firms.

6.3 Out of sample analysis

In addition to the Granger causality tests, we apply the sg-LASSO-MIDAS model to predict the earnings forecast errors and test whether machine learning can improve upon analysts' predictions. As we aim at predicting the earnings forecast errors, we test whether machine learning methods can generate accurate out-of-sample forecasts to correct analysts' forecasts and thereby improve the overall performance.

We split the full sample into two halves, estimate the sg-LASSO-MIDAS model as in equation (9) based on the first half of the time-series observations and generate the forecasts. We then reestimate the model parameters based on the expanding window scheme and use the real-time data updates for macroeconomic variables. We use the 5-fold cross-validation to compute the tuning parameters. The results appear in Table 5.

We find that machine learning can indeed predict and correct the forecast errors made by analysts. When using the full set of covariates, the sg-LASSO-MIDAS model reduces the earnings forecast errors by 3%. We find further reduction in earnings forecast errors by 4% when only using the covariates which we find to be significant, see Table 3 Panel (B). The gain in prediction quality is significant at the 5% level based on the Diebold and Mariano (1995) test in both cases. Overall, the results appear to indicate that model-based predictions can significantly improve earnings forecasts when combined with the analysts predictions.

7 Conclusions

This paper introduced a new class of high-dimensional panel data regression models with dictionaries and sg-LASSO regularization. This type of regularization is an especially attractive choice for predictive panel data regressions, where the low- and/or the high-frequency lags define a clear group structure. The estimator nests the LASSO and the group LASSO estimators as special cases. Our theoretical treatment allows for heavy-tailed data frequently encountered in financial time series. To that end, we obtain a new panel data concentration inequality of the Fuk-Nagaev type for τ-mixing processes, which allows us to establish oracle inequalities that are used subsequently to develop the debiased HAC inference for the panel data sg-LASSO estimator.

Using the theory of HAC-based inference for pooled panel data regressions developed in our paper, our empirical analysis revisits a topic raised by earlier literature that analysts tend to focus on firm and/or industry information when forming earnings forecasts, while not fully taking into account the macroeconomic data. Our results suggest that indeed analysts tend to miss on macro information, i.e., macro variables turn out to be significant in pooled panel regression models.

	id		Frequency	Source	T-code
		Firm-level series			
		Panel A1.			
-	Earnings		quarterly	CRSP & I/B/E/S	1
-	Earnings consensus forecasts		quarterly	CRSP & I/B/E/S	1
-	Other earnings/earnings forecast implied series		quarterly	CRSP & I/B/E/S	1
		Panel B1.			
1	Stock returns		daily	CRSP	1
2	Realized variance measure		daily	CRSP/computations	1
		Panel C1.			
3	Event Sentiment Score (ESS)		daily	RavenPack	1
4	Aggregate Event Sentiment (AES)		daily	RavenPack	1
5	Aggregate Event Volume (AEV)		daily	RavenPack	1
6	Composite Sentiment Score (CSS)		daily	RavenPack	1
7	News Impact Projections (NIP)		daily	RavenPack	1
		Other series			
		Panel A2.			
8	Industrial Production Index		monthly	ALFRED	3
9	CPI inflation		monthly	ALFRED	4
10	Unemployment rate		monthly	ALFRED	1
11	Real GDP		quarterly	ALFRED	2
		Panel B2.			
12	Crude Oil Prices		daily	FRED	4
13	S&P 500		daily	CRSP	3
14	VIX Volatility Index		daily	FRED	1
15	Moodys Aaa less 10-Year Treasury		daily	FRED	1
16	Moodys Baa less 10-Year Treasury		daily	FRED	1
17	Moodys Baa less Aaa (corporate yield spread)		daily	FRED	1
18	10-Year Treasury minus 3-Month Treasury (term spread)		daily	FRED	1
19	3-Month Treasury minus Effective Federal funds rate (short-term spread)		daily	FRED	1
20	TED rate		daily	FRED	1
		Panel C2.			
21	Earnings		monthly	Bybee, Kelly, Manela, and Xiu (2019)	1
22	Earnings forecasts		monthly	Bybee, Kelly, Manela, and Xiu (2019)	1
23	Earnings losses		monthly	Bybee, Kelly, Manela, and Xiu (2019)	1
24	Recession		monthly	Bybee, Kelly, Manela, and Xiu (2019)	1
25	Revenue growth		monthly	Bybee, Kelly, Manela, and Xiu (2019)	1
26	Revised estimate		monthly	Bybee, Kelly, Manela, and Xiu (2019)	1

Table 2: Firm-level data description table — The *id* column gives mnemonics according to data source, which is given in the second column *Source*. The column *frequency* states the sampling frequency of the variable. The column *T-code* denotes the data transformations applied to a time series, which are (1) not transformed, (2) $100[(x_t/x_{t-1})^4 - 1]$, (3) $\Delta \log(x_t)$, (4) $\Delta^2 \log(x_t)$. The block of firm-level series contains three panels: A1 – describes earnings data, B1 – describes daily firm-level stock market data, and C1 – describes daily firm-level sentiment data series. The block labeled "other series" also has three panels: A2 – describes real-time monthly macro series, B2 – describes daily financial markets data, and C2 – describes monthly news attention series. In the models we include 365 daily lags, 12 monthly lags and 4 quarterly lags respectively.

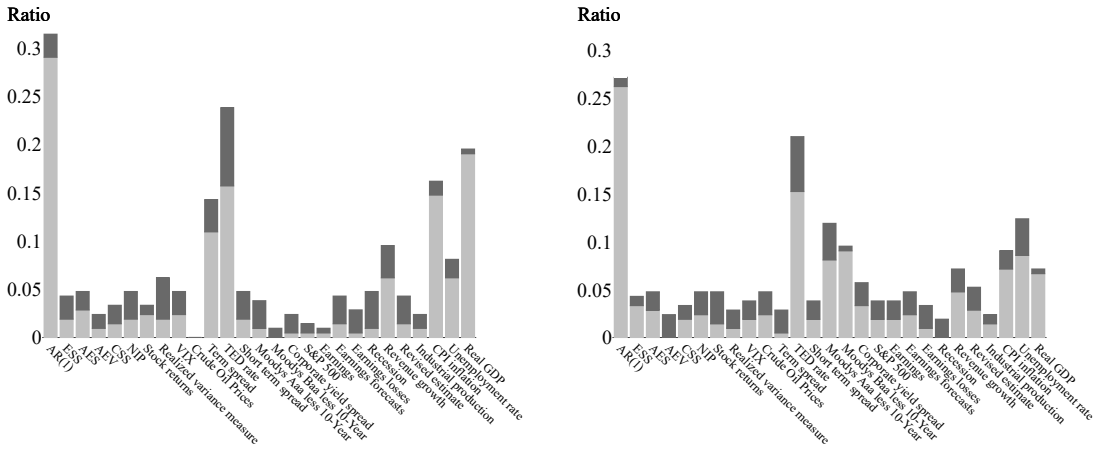

(a) sg-LASSO-MIDAS (b) LASSO-UMIDAS

Figure 1: Individual regression-based Granger causality tests. In Panel (a) we plot the ratios based on sg-LASSO estimator and MIDAS weighting scheme with Legendre polynomials, while in Panel (b) we plot for the ratios for the standard LASSO estimator with UMIDAS weighting scheme. The lighter-gray color shows the ratio for firms with high disagreement, while the dark-gray color shows the ratio for firms with low disagreement; see Table 4. All results are based on the 5% significance level.

Variable $\backslash M_T$	10	20	30	10	20	30
	Quadratic Spectral			Parzen		
	Panel (A) – AR(1)					
AR(1)	0.001	0.000	0.000	0.002	0.001	0.001
	Panel (B) – sg-LASSO					
	Significant variables at 5% or less					
AR(1)	0.001	0.000	0.000	0.002	0.001	0.000
TED rate	0.001	0.001	0.000	0.003	0.001	0.001
CPI inflation	0.003	0.001	0.001	0.013	0.003	0.001
Real GDP	0.028	0.003	0.001	0.035	0.021	0.006
	Significant variables at 10% level					
Term spread	0.012	0.014	0.023	0.053	0.016	0.015
	Panel (C) – LASSO (significant for sg-LASSO)					
	Significant variables at 5% or less					
AR(1)	0.001	0.000	0.000	0.002	0.001	0.000
TED rate	0.000	0.000	0.000	0.000	0.000	0.000
CPI inflation	0.677	0.390	0.461	0.651	0.724	0.576
Real GDP	0.341	0.247	0.094	0.339	0.328	0.270
	Significant variables at 10% level					
Term spread	0.273	0.060	0.022	0.235	0.387	0.365
	LASSO (significant only for LASSO)					
	Significant variables at 5% or less					
AAA less 10 year	0.009	0.001	0.001	0.015	0.014	0.007
BAA less 10 year	0.000	0.000	0.000	0.000	0.000	0.000

Table 3: Significance testing results — We report p-values for the AR(1) in Panel (A) and for the sg-LASSO using the MIDAS scheme with Legendre polynomials in Panel (B) displaying series significant at the 5% or 10% significance level. We also report results for the standard LASSO estimator together with the UMIDAS scheme in Panel (C). The results are reported for a range of bandwidth parameters (M_T = 10, 20 and 30) and two kernel functions (Quadratic Spectral and Parzen).

Variable $\backslash M_T$	10	20	30	10	20	30
	Quadratic Spectral			Parzen		
	Large disagreement					
	Significant variables at 5% or less					
AR(1)	0.002	0.001	0.000	0.004	0.001	0.001
Term spread	0.029	0.023	0.016	0.085	0.036	0.026
TED rate	0.002	0.001	0.001	0.016	0.002	0.001
CPI inflation	0.016	0.009	0.007	0.040	0.018	0.011
	Significant variables at 10% level					
Real GDP	0.098	0.005	0.000	0.098	0.082	0.021
	Small disagreement					
	Significant variables at 5% or less					
AR(1)	0.000	0.000	0.000	0.000	0.000	0.000
Stock returns	0.008	0.004	0.003	0.015	0.008	0.006
	Significant variables at 10% level					
Unemployment rate	0.060	0.043	0.045	0.060	0.056	0.048

Table 4: Significance testing results — We report p-values for the AR(1) and for the sg-LASSO-MIDAS models, displaying series significant at the 5% or 10% significance level. The results are reported for a range of bandwidth parameters and two kernel functions. We pool the response based on large versus small disagreement, which we measure as the average (over time series) of the difference between 95% and 5% percentile of the empirical forecast distribution of the analysts.

	MSE ratio	DM statistic
All covariates	0.968	1.986
Significant covariates	0.960	2.143

Table 5: Out of sample prediction results — We report one-quarter ahead real-time out-of-sample forecasting results. In the first row we report results based on a full set of covariates, while in the second row the results are based on covariates which we find to be significant, see Table 3 Panel (B). We report the mean-squared-error ratio (column (MSE ratio) of sg-LASSO-MIDAS model corrected prediction relative to the analyst-only prediction of earnings. The last column reports the Diebold and Mariano (1995) test statistic.

References

Almon, S. (1965): "The distributed lag between capital appropriations and expenditures," *Econometrica*, 33(1), 178–196.

Alvarez, J., and M. Arellano (2003): "The time series and cross-section asymptotics of dynamic panel data estimators," *Econometrica*, 71(4), 1121–1159.

Apostol, T. M. (1974): *Mathematical analysis*. Pearson.

Arellano, M. (2003): *Panel data econometrics*. Oxford University Press.

Babii, A. (2021): "High-dimensional mixed-frequency IV regression," *Journal of Business and Economic Statistics* (forthcoming).

Babii, A., and J.-P. Florens (2020): "Is completeness necessary? Estimation in nonidentified linear models," Mimeo-UNC Chapel Hill.

Babii, A., E. Ghysels, and J. Striaukas (2022a): "High-dimensional Granger causality tests with an application to VIX and news," *Journal of Financial Econometrics* (forthcoming).

——— (2022b): "Machine learning time series regressions with an application to nowcasting," *Journal of Business and Economic Statistics*, 40, 1094–1106.

Ball, R. T., and P. Easton (2013): "Dissecting earnings recognition timeliness," *Journal of Accounting Research*, 51(5), 1099–1132.

Ball, R. T., and L. A. Gallo (2018): "A mixed data sampling approach to accounting research," available at SSRN 3250445.

Ball, R. T., and E. Ghysels (2018): "Automated earnings forecasts: beat analysts or combine and conquer?," *Management Science*, 64(10), 4936–4952.

Belloni, A., M. Chen, O. H. M. Padilla, et al. (2019): "High dimensional latent panel quantile regression with an application to asset pricing," *arXiv preprint arXiv:1912.02151*.

Belloni, A., V. Chernozhukov, C. Hansen, and D. Kozbur (2016): "Inference in high-dimensional panel models with an application to gun control," *Journal of Business and Economic Statistics*, 34(4), 590–605.

Billingsley, P. (1995): *Probability and measure*. John Wiley & Sons.

Bybee, L., B. T. Kelly, A. Manela, and D. Xiu (2019): "The structure of economic news," available at SSRN 3446225.

Carabias, J. M. (2018): "The real-time information content of macroeconomic news: implications for firm-level earnings expectations," *Review of Accounting Studies*, 23(1), 136–166.

Carrasco, M., J.-P. Florens, and E. Renault (2007): "Linear inverse problems in structural econometrics estimation based on spectral decomposition and regularization," in *Handbook of Econometrics - Volume 6B*, ed. by J. J. Heckman, and E. E. Leamer, pp. 5633–5751. Elsevier.

Chernozhukov, V., J. A. Hausman, and W. K. Newey (2019): "Demand analysis with many prices," National Bureau of Economic Research Discussion paper 26424.

Chiang, H. D., J. Rodrigue, and Y. Sasaki (2019): "Post-selection inference in three-dimensional panel data," *arXiv preprint arXiv:1904.00211*.

Dedecker, J., and P. Doukhan (2003): "A new covariance inequality and applications," *Stochastic Processes and their Applications*, 106(1), 63–80.

Dedecker, J., and C. Prieur (2004): "Coupling for τ-dependent sequences and applications," *Journal of Theoretical Probability*, 17(4), 861–885.

——— (2005): "New dependence coefficients. Examples and applications to statistics," *Probability Theory and Related Fields*, 132(2), 203–236.

Diebold, F. X., and R. S. Mariano (1995): "Comparing predictive accuracy," *Journal of Business and Economic Statistics*, 13(3), 253–263.

Farrell, M. H. (2015): "Robust inference on average treatment effects with possibly more covariates than observations," *Journal of Econometrics*, 189(1), 1–23.

Fernández-Val, I., and M. Weidner (2016): "Individual and time effects in nonlinear panel models with large N, T," *Journal of Econometrics*, 192(1), 291–312.

Foroni, C., M. Marcellino, and C. Schumacher (2015): "Unrestricted mixed data sampling (MIDAS): MIDAS regressions with unrestricted lag polynomials," *Journal of the Royal Statistical Society: Series A (Statistics in Society)*, 178(1), 57–82.

Fuk, D. K., and S. V. Nagaev (1971): "Probability inequalities for sums of independent random variables," *Theory of Probability and Its Applications*, 16(4), 643–660.

Ghysels, E., and H. Qian (2019): "Estimating MIDAS regressions via OLS with polynomial parameter profiling," *Econometrics and Statistics*, 9, 1–16.

Ghysels, E., P. Santa-Clara, and R. Valkanov (2006): "Predicting volatility: getting the most out of return data sampled at different frequencies," *Journal of Econometrics*, 131(1–2), 59–95.

Ghysels, E., A. Sinko, and R. Valkanov (2006): "MIDAS regressions: further results and new directions," *Econometric Reviews*, 26(1), 53–90.

——— (2007): "MIDAS regressions: further results and new directions," *Econometric Reviews*, 26(1), 53–90.

Hahn, J., and G. Kuersteiner (2002): "Asymptotically unbiased inference for a dynamic panel model with fixed effects when both n and T are large," *Econometrica*, 70(4), 1639–1657.

Hansen, C. B. (2007): "Asymptotic properties of a robust variance matrix estimator for panel data when T is large," *Journal of Econometrics*, 141(2), 597–620.

Harding, M., and C. Lamarche (2019): "A panel quantile approach to attrition bias in Big Data: Evidence from a randomized experiment," *Journal of Econometrics*, 211(1), 61–82.

Khalaf, L., M. Kichian, C. J. Saunders, and M. Voia (2021): "Dynamic panels with MIDAS covariates: nonlinearity, estimation and fit," *Journal of Econometrics*, 220(2), 589–605.

Kock, A. B. (2013): "Oracle efficient variable selection in random and fixed effects panel data models," *Econometric Theory*, 29(1), 115–152.

——— (2016): "Oracle inequalities, variable selection and uniform inference in high-dimensional correlated random effects panel data models," *Journal of Econometrics*, 195(1), 71–85.

Koenker, R. (2004): "Quantile regression for longitudinal data," *Journal of Multivariate Analysis*, 91(1), 74–89.

Kolanovic, M., and R. Krishnamachari (2017): "Big data and AI strategies: Machine learning and alternative data approach to investing," JP Morgan Global Quantitative & Derivatives Strategy Report.

Lamarche, C. (2010): "Robust penalized quantile regression estimation for panel data," *Journal of Econometrics*, 157(2), 396–408.

Lu, X., and L. Su (2016): "Shrinkage estimation of dynamic panel data models with interactive fixed effects," *Journal of Econometrics*, 190(1), 148–175.

Marsilli, C. (2014): "Variable selection in predictive MIDAS models," *Banque de France Working Paper*.

Phillips, P. C. B., and H. R. Moon (1999): "Linear regression limit theory for nonstationary panel data," *Econometrica*, 67(5), 1057–1111.

Simon, N., J. Friedman, T. Hastie, and R. Tibshirani (2013): "A sparse-group LASSO," *Journal of Computational and Graphical Statistics*, 22(2), 231–245.

Su, L., Z. Shi, and P. C. B. Phillips (2016): "Identifying latent structures in panel data," *Econometrica*, 84(6), 2215–2264.

APPENDIX

A Proofs

Proof of Theorem 3.1. By Fermat's rule, the pooled sg-LASSO satisfies

$$\mathbf{Z}^\top(\mathbf{Z}\hat{\rho} - \mathbf{y})/NT + \lambda z^* = 0_{p+1}$$

for some $z^* \in \partial\Omega(\hat{\rho})$, where $\partial\Omega(\hat{\rho})$ is the subdifferential of $b \mapsto \Omega(b)$ at $\hat{\rho}$. Taking the inner product with $\rho - \hat{\rho}$

$$\begin{aligned}\langle \mathbf{Z}^\top(\mathbf{y} - \mathbf{Z}\hat{\rho}), \rho - \hat{\rho}\rangle_{NT} &= \lambda\langle z^*, \rho - \hat{\rho}\rangle \\ &\leq \lambda\left\{\Omega(\rho) - \Omega(\hat{\rho})\right\},\end{aligned}$$

where the last line follows from the definition of the subdifferential. Since $\mathbf{y} = \mathbf{m} + \mathbf{u}$, the inequality can be rewritten as

$$\begin{aligned}\|\mathbf{Z}(\hat{\rho} - \rho)\|_{NT}^2 - \lambda\left\{\Omega(\rho) - \Omega(\hat{\rho})\right\} &\leq \langle \mathbf{Z}^\top(\mathbf{Z}\rho - \mathbf{y}), \rho - \hat{\rho}\rangle_{NT} \\ &= \langle \mathbf{Z}^\top\mathbf{u}, \hat{\rho} - \rho\rangle_{NT} + \langle \mathbf{m} - \mathbf{Z}\rho, \mathbf{Z}(\hat{\rho} - \rho)\rangle_{NT}.\end{aligned}$$

By the dual norm inequality $\langle \mathbf{Z}^\top\mathbf{u}, \hat{\rho} - \rho\rangle_{NT} \leq \Omega^*(\mathbf{Z}^\top\mathbf{u}/NT)\Omega(\hat{\rho} - \rho)$, where Ω^* is the dual norm of Ω. Then by Babii, Ghysels, and Striaukas (2022b), Lemma A.2.1

$$\begin{aligned}\Omega^*(\mathbf{Z}^\top\mathbf{u}/NT) &\leq \gamma|\mathbf{Z}^\top\mathbf{u}/NT|_\infty + (1-\gamma)\max_{G\in\mathcal{G}}|\mathbf{Z}_G^\top\mathbf{u}/NT|_2 \\ &\leq \max_{G\in\mathcal{G}}\sqrt{|G|}|\mathbf{Z}^\top\mathbf{u}/NT|_\infty \\ &\leq \lambda/c,\end{aligned}$$

where the last line follows from Theorem A.1 with probability at least $1-\delta$ and Assumption 3.3 for some $c > 1$. Therefore,

$$\|\mathbf{Z}\Delta\|_{NT}^2 - \lambda\left\{\Omega(\rho) - \Omega(\hat{\rho})\right\} \leq \frac{\lambda}{c}\Omega(\Delta) + \|\mathbf{m} - \mathbf{Z}\rho\|_{NT}\|\mathbf{Z}\Delta\|_{NT} \text{ with } \Delta = \hat{\rho} - \rho. \quad \text{(A.1)}$$

Note that the sg-LASSO penalty function can be decomposed as a sum of two semi-norms $\Omega(r) = \Omega_0(r) + \Omega_1(r), \forall r \in \mathbf{R}^{1+p}$ with

$$\Omega_0(r) = \gamma|r_{S_0}|_1 + (1-\gamma)\sum_{G\in\mathcal{G}_0}|r_G|_2 \quad \text{and} \quad \Omega_1(r) = \gamma|r_{S_0^c}|_1 + (1-\gamma)\sum_{G\in\mathcal{G}_0^c}|r_G|_2.$$

Note also that $\Omega_1(\rho) = 0$ and $\Omega_1(\hat{\rho}) = \Omega_1(\hat{\rho} - \rho)$. Then

$$\begin{aligned}\Omega(\rho) - \Omega(\hat{\rho}) &= \Omega_0(\rho) - \Omega_0(\hat{\rho}) - \Omega_1(\hat{\rho}) \\ &\leq \Omega_0(\hat{\rho} - \rho) - \Omega_1(\hat{\rho} - \rho) = \Omega_0(\Delta) - \Omega_1(\Delta).\end{aligned} \quad \text{(A.2)}$$

Suppose that $\|\mathbf{m} - \mathbf{Z}\rho\|_{NT} \leq \frac{1}{2}\|\mathbf{Z}\Delta\|_{NT}$. Then it follows from equations (A.1) and (A.2) that

$$\begin{aligned}\|\mathbf{Z}\Delta\|_{NT}^2 &\leq 2\frac{\lambda}{c}\Omega(\Delta) + 2\lambda\left\{\Omega_0(\Delta) - \Omega_1(\Delta)\right\} \\ &= 2\frac{\lambda}{c}\left\{\Omega_1(\Delta) + \Omega_0(\Delta)\right\} + 2\lambda\left\{\Omega_0(\Delta) - \Omega_1(\Delta)\right\}\end{aligned}$$

Since the left side of this equation is greater or equal to zero, this shows that

$$\Omega_1(\Delta) \leq \frac{c+1}{c-1}\Omega_0(\Delta). \tag{A.3}$$

Put $\Sigma_{N,T} = \frac{1}{NT}\sum_{i=1}^{N}\sum_{t=1}^{T}\mathbb{E}[z_{i,t}z_{i,t}^\top]$. Therefore,

$$\begin{aligned}\Omega(\Delta) &\leq \frac{2c}{c-1}\Omega_0(\Delta) \leq \frac{2c}{c-1}\sqrt{s|\Delta|_2^2} \leq \frac{2c}{c-1}\sqrt{\frac{s}{\gamma_{\min}}|\Sigma_{N,T}^{1/2}\Delta|_2^2} \\ &= \frac{2c}{c-1}\sqrt{\frac{s}{\gamma_{\min}}\left\{\|\mathbf{Z}\Delta\|_{NT}^2 + \Delta^\top(\hat{\Sigma} - \Sigma_{N,T})\Delta\right\}} \\ &\leq \frac{2c}{c-1}\sqrt{\frac{s}{\gamma_{\min}}\left\{\|\mathbf{Z}\Delta\|_{NT}^2 + \Omega(\Delta)\Omega^*((\hat{\Sigma} - \Sigma_{N,T})\Delta)\right\}} \\ &\leq \frac{2c}{c-1}\sqrt{\frac{s}{\gamma_{\min}}\left\{2(1+c^{-1})\lambda\Omega(\Delta) + \Omega^2(\Delta)G^*|\mathrm{vech}(\hat{\Sigma} - \Sigma_{N,T})|_\infty\right\}},\end{aligned}$$

where we set $G^* = \max_{G\in\mathcal{G}}\sqrt{|G|}$ and use Hölder's inequality, inequalities in equations (A.1) and (A.3), Assumption 3.2, $\hat{\Sigma} = \mathbf{Z}^\top\mathbf{Z}/NT$, and Babii, Ghysels, and Striaukas (2022b), Lemma A.2.1. This shows that with probability at least $1-\delta$

$$\Omega(\Delta) \leq \frac{4c^2 s}{(c-1)^2\gamma_{\min}}\left\{2(1+c^{-1})\lambda + \Omega(\Delta)G^*|\mathrm{vech}(\hat{\Sigma} - \Sigma_{N,T})|_\infty\right\}. \tag{A.4}$$

Consider the following event $E = \{|\mathrm{vech}(\hat{\Sigma} - \Sigma_{N,T})|_\infty < (2c^*G^*s)^{-1}\}$ with $c^* = (3c+1)^2/(\gamma_{\min}(c-1)^2)$, and note that under Assumption 3.1 by Theorem A.1

$$\begin{aligned}\Pr(E^c) &= \Pr\left(\max_{1\leq j\leq k\leq p}\left|\frac{1}{NT}\sum_{i=1}^{N}\sum_{t=1}^{T}z_{i,t,j}z_{i,t,k} - \mathbb{E}[z_{i,t,j}z_{i,t,k}]\right| \geq \frac{1}{2c^*G^*s}\right) \\ &\lesssim p^2(NT)^{1-\tilde{\kappa}}s^{\tilde{\kappa}} + p^2e^{-cNT/s^2}\end{aligned}$$

for some $c > 0$. On the event E, the inequality in equation (A.4) implies $\Omega(\Delta) \lesssim s\lambda$, and whence from the equation (A.1) by the triangle inequality

$$\|\mathbf{Z}\Delta\|_{NT}^2 \leq 2(1+c^{-1})\lambda\Omega(\Delta) \lesssim s\lambda^2.$$

Therefore, we obtain the statement of the theorem as long as $\|\mathbf{m} - \mathbf{Z}\rho\|_{NT} \leq \frac{1}{2}\|\mathbf{Z}\Delta\|_{NT}$. Suppose now that $\|\mathbf{m} - \mathbf{Z}\rho\|_{NT} > \frac{1}{2}\|\mathbf{Z}\Delta\|_{NT}$. Then

$$\|\mathbf{Z}\Delta\|_{NT}^2 \leq 4\|\mathbf{m} - \mathbf{Z}\rho\|_{NT}^2.$$

Therefore, the first statement of the theorem always holds with probability at least $1 - \delta - O(r_{N,T}^{\text{pooled}})$

$$\|\mathbf{Z}\Delta\|_{NT}^2 \lesssim s\lambda^2 + \|\mathbf{m} - \mathbf{Z}\rho\|_{NT}^2.$$

For the second statement, suppose first that

$$\Omega_1(\Delta) \leq 2\frac{c+1}{c-1}\Omega_0(\Delta). \tag{A.5}$$

Then by the same arguments as before, on the event E, we have

$$\begin{aligned}
\Omega(\Delta) &\leq \left(1 + 2\frac{c+1}{c-1}\right)\Omega_0(\Delta) \\
&\leq \frac{3c+1}{c-1}\sqrt{\frac{s}{\gamma_{\min}}\left\{\|\mathbf{Z}\Delta\|_{NT}^2 + \frac{1}{2c^* s}\Omega^2(\Delta)\right\}} \\
&= \sqrt{\frac{(3c+1)^2}{(c-1)^2\gamma_{\min}}s\|\mathbf{Z}\Delta\|_{NT}^2 + \frac{1}{2}\Omega^2(\Delta)}
\end{aligned}$$

or simply

$$\Omega(\Delta) \leq \sqrt{2}\frac{(3c+1)}{(c-1)}\sqrt{\frac{s}{\gamma_{\min}}}\|\mathbf{Z}\Delta\|_{NT} \lesssim s\lambda + \sqrt{s}\|\mathbf{m} - \mathbf{Z}\rho\|_{NT},$$

where we use the first statement of the theorem. On the other hand, if the inequality in equation (A.5) does not hold, then the inequality in equation (A.3) also does not hold, which implies that

$$\|\mathbf{m} - \mathbf{Z}\rho\|_{NT} > \frac{1}{2}\|\mathbf{Z}\Delta\|_{NT}.$$

Then since $\|\mathbf{Z}\Delta\|_{NT} \geq 0$ from (A.1) we obtain

$$\begin{aligned}
0 &\leq \frac{1}{c}\Omega(\Delta) + \Omega(\rho) - \Omega(\hat{\rho}) + \frac{2}{\lambda}\|\mathbf{m} - \mathbf{Z}\rho\|_{NT}^2 \\
&\leq \frac{1}{c}\Omega(\Delta) + \Omega_0(\Delta) - \Omega_1(\Delta) + \frac{2}{\lambda}\|\mathbf{m} - \mathbf{Z}\rho\|_{NT}^2,
\end{aligned}$$

where we use equation (A.2). Since $\Omega(\Delta) = \Omega_1(\Delta) + \Omega_0(\Delta)$

$$\begin{aligned}
\Omega_1(\Delta) &\leq \frac{c+1}{c-1}\Omega_0(\Delta) + \frac{2c}{\lambda(c-1)}\|\mathbf{m} - \mathbf{Z}\rho\|_{NT}^2 \\
&\leq \frac{1}{2}\Omega_1(\Delta) + \frac{2c}{\lambda(c-1)}\|\mathbf{m} - \mathbf{Z}\rho\|_{NT}^2,
\end{aligned}$$

where we use the fact that the inequality in equation (A.5) does not hold. Therefore,

$$\Omega_1(\Delta) \leq \frac{4c}{\lambda(c-1)} \|\mathbf{m} - \mathbf{Z}\rho\|_{NT}^2,$$

which shows that

$$\Omega(\Delta) \lesssim \Omega_1(\Delta) \leq \frac{4c}{\lambda(c-1)} \|\mathbf{m} - \mathbf{Z}\rho\|_{NT}^2.$$

Therefore, with probability at least $1 - \delta - O(r_{N,T}^{\text{pooled}})$, we always have

$$\Omega(\Delta) \lesssim s\lambda + \sqrt{s}\|\mathbf{m} - \mathbf{Z}\rho\|_{NT} + \frac{1}{\lambda}\|\mathbf{m} - \mathbf{Z}\rho\|_{NT}^2.$$

The result follows from the equivalence between Ω and $|.|_1$ norms provided that groups have fixed size. □

Proof of Theorem 3.2. By Fermat's rule the solution to the fixed effects regression satisfies

$$\mathbf{Z}^\top(\mathbf{Z}\hat{\rho} - \mathbf{y})/NT + \lambda z^* = 0_{N+p}, \text{ for some } z^* = \begin{pmatrix} 0_N \\ z_b^* \end{pmatrix},$$

where 0_N is N-dimensional vector of zeros, $z_b^* \in \partial\Omega(\hat{\beta})$, $\hat{\rho} = (\hat{\alpha}^\top, \hat{\beta}^\top)^\top$, and $\partial\Omega(\hat{\beta})$ is the sub-differential of $b \mapsto \Omega(b)$ at $\hat{\beta}$. Taking the inner product with $\rho - \hat{\rho}$

$$\begin{aligned}\langle \mathbf{Z}^\top(\mathbf{y} - \mathbf{Z}\hat{\rho}), \rho - \hat{\rho}\rangle_{NT} &= \lambda\langle z^*, \rho - \hat{\rho}\rangle \\ &= \lambda\langle z_b^*, \beta - \hat{\beta}\rangle \leq \lambda\left\{\Omega(\beta) - \Omega(\hat{\beta})\right\},\end{aligned}$$

where the last line follows from the definition of the sub-differential. Rearranging this inequality and using $\mathbf{y} = \mathbf{m} + \mathbf{u}$

$$\begin{aligned}\|\mathbf{Z}(\hat{\rho} - \rho)\|_{NT}^2 - \lambda\left\{\Omega(\beta) - \Omega(\hat{\beta})\right\} \leq& \langle \mathbf{Z}^\top\mathbf{u}, \hat{\rho} - \rho\rangle_{NT} + \langle \mathbf{Z}^\top(\mathbf{m} - \mathbf{Z}\rho), \hat{\rho} - \rho\rangle_{NT} \\ \leq& \langle B^\top\mathbf{u}, \hat{\alpha} - \alpha\rangle_{NT} + \langle \mathbf{X}^\top\mathbf{u}, \hat{\beta} - \beta\rangle_{NT} \\ &+ \|\mathbf{m} - \mathbf{Z}\rho\|_{NT}\|\mathbf{Z}(\hat{\rho} - \rho)\|_{NT} \\ \leq& |B^\top\mathbf{u}/NT|_\infty|\hat{\alpha} - \alpha|_1 + \Omega^*(\mathbf{X}^\top\mathbf{u}/NT)\Omega(\hat{\beta} - \beta) \\ &+ \|\mathbf{m} - \mathbf{Z}\rho\|_{NT}\|\mathbf{Z}(\hat{\rho} - \rho)\|_{NT} \\ \leq& |B^\top\mathbf{u}/\sqrt{NT}|_\infty \vee \Omega^*(\mathbf{X}^\top\mathbf{u}/NT) \\ &\times \left\{|\hat{\alpha} - \alpha|_1/\sqrt{N} + \Omega(\hat{\beta} - \beta)\right\} \\ &+ \|\mathbf{m} - \mathbf{Z}\rho\|_{NT}\|\mathbf{Z}(\hat{\rho} - \rho)\|_{NT},\end{aligned} \tag{A.6}$$

where the second line follows by the dual norm inequality and the Cauchy-Schwartz inequality, and Ω^* is the dual norm of Ω. By Babii, Ghysels, and Striaukas (2022b), Lemma A.2.1. and Theorem A.1 under Assumption 3.1, with probability at least $1-\delta/2$

$$\Omega^*(\mathbf{X}^\top \mathbf{u}/NT) \leq \max_{G\in\mathcal{G}} \sqrt{|G|}|\mathbf{X}^\top \mathbf{u}/NT|_\infty \lesssim \left(\frac{p}{\delta(NT)^{\kappa-1}}\right)^{1/\kappa} \vee \sqrt{\frac{\log(16p/\delta)}{NT}}.$$

Similarly, under Assumption 3.1 by Babii, Ghysels, and Striaukas (2022a), Theorem 3.1 with probability at least $1-\delta/2$

$$|B^\top \mathbf{u}/\sqrt{N}T|_\infty = \max_{i\in[N]} \left|\frac{1}{\sqrt{N}T}\sum_{t=1}^{T} u_{i,t}\right| \lesssim \left(\frac{N}{\delta N^{\kappa/2}T^{\kappa-1}}\right)^{1/\kappa} \vee \sqrt{\frac{\log(16N/\delta)}{NT}}.$$

Therefore, under Assumption 3.5 with probability at least $1-\delta$

$$|B^\top \mathbf{u}/NT|_\infty \vee \Omega^*(\mathbf{X}^\top \mathbf{u}/NT) \lesssim \left(\frac{(pN^{1-\kappa}) \vee N^{1-\kappa/2}}{\delta T^{\kappa-1}}\right)^{1/\kappa} \vee \sqrt{\frac{\log(p\vee N/\delta)}{NT}} \lesssim \lambda.$$

In conjunction with the inequality in equation (A.6), this gives

$$\begin{aligned}\|\mathbf{Z}\Delta\|_{NT}^2 &\leq c^{-1}\lambda\left\{|\hat{\alpha}-\alpha|_1/\sqrt{N} + \Omega(\hat{\beta}-\beta)\right\} \\ &\quad + \|\mathbf{m}-\mathbf{Z}\rho\|_{NT}\|\mathbf{Z}\Delta\|_{NT} + \lambda\left\{\Omega(\beta)-\Omega(\hat{\beta})\right\} \\ &\leq (c^{-1}+1)\lambda\left\{|\hat{\alpha}-\alpha|_1/\sqrt{N} + \Omega(\hat{\beta}-\beta)\right\} + \|\mathbf{m}-\mathbf{Z}\rho\|_{NT}\|\mathbf{Z}\Delta\|_{NT}\end{aligned} \tag{A.7}$$

for some $c>1$ and $\Delta = \hat{\rho}-\rho$, where the second line follows by the triangle inequality. Note that the sg-LASSO penalty function can be decomposed as a sum of two semi-norms $\Omega(b) = \Omega_0(b) + \Omega_1(b), \forall b \in \mathbf{R}^p$ with

$$\Omega_0(b) = \gamma|b_{S_0}|_1 + (1-\gamma)\sum_{G\in\mathcal{G}_0}|b_G|_2 \quad \text{and} \quad \Omega_1(b) = \gamma|b_{S_0^c}|_1 + (1-\gamma)\sum_{G\in\mathcal{G}_0^c}|b_G|_2.$$

Note also that $\Omega_1(\beta)=0$ and $\Omega_1(\hat{\beta}) = \Omega_1(\hat{\beta}-\beta)$. Then

$$\begin{aligned}\Omega(\beta)-\Omega(\hat{\beta}) &= \Omega_0(\beta)-\Omega_0(\hat{\beta})-\Omega_1(\hat{\beta}) \\ &\leq \Omega_0(\hat{\beta}-\beta)-\Omega_1(\hat{\beta}-\beta).\end{aligned} \tag{A.8}$$

Suppose that $\|\mathbf{m}-\mathbf{Z}\rho\|_{NT} \leq \frac{1}{2}\|\mathbf{Z}\Delta\|_{NT}$. Then from the first inequality in equation (A.7) and equation (A.2), we obtain

$$\|\mathbf{Z}\Delta\|_{NT}^2 \leq 2c^{-1}\lambda\left\{|\hat{\alpha}-\alpha|_1/\sqrt{N} + \Omega(\hat{\beta}-\beta)\right\} + 2\lambda\left\{\Omega_0(\hat{\beta}-\beta)-\Omega_1(\hat{\beta}-\beta)\right\}.$$

Since the left side of this equation is ≥ 0, this shows that

$$(1-c^{-1})\Omega_1(\hat{\beta}-\beta) \leq (1+c^{-1})\Omega_0(\hat{\beta}-\beta) + c^{-1}|\hat{\alpha}-\alpha|_1/\sqrt{N}$$

or equivalently

$$\Omega_1(\hat{\beta}-\beta) \leq \frac{c+1}{c-1}\Omega_0(\hat{\beta}-\beta) + (c-1)^{-1}|\hat{\alpha}-\alpha|_1/\sqrt{N}. \tag{A.9}$$

Put $\Delta_N = ((\hat{\alpha}-\alpha)^\top/\sqrt{N}, (\hat{\beta}-\beta)^\top)^\top$. Then under Assumption 3.2

$$\begin{aligned}
|\Delta_N|_1 &\lesssim \Omega(\hat{\beta}-\beta) + |\hat{\alpha}-\alpha|_1/\sqrt{N} \\
&\leq \frac{2c}{c-1}\Omega_0(\hat{\beta}-\beta) + \frac{c}{c-1}|\hat{\alpha}-\alpha|_1/\sqrt{N} \\
&\lesssim |\hat{\alpha}-\alpha|_2 + \sqrt{s}|\hat{\beta}-\beta|_2 \\
&\leq \sqrt{s\vee N|\Delta_N|_2^2} \\
&\lesssim \sqrt{s\vee N|\Sigma^{1/2}\Delta_N|_2^2} \\
&= \sqrt{s\vee N\left\{\|\mathbf{Z}\Delta\|_{NT}^2 + \Delta_N^\top(\hat{\Sigma}-\Sigma)\Delta_N\right\}} \\
&\leq \sqrt{s\vee N\left\{\|\mathbf{Z}\Delta\|_{NT}^2 + |\Delta_N|_1^2|\mathrm{vech}(\hat{\Sigma}-\Sigma)|_\infty\right\}} \\
&\lesssim \sqrt{s\vee N\left\{\lambda|\Delta_N|_1 + |\Delta_N|_1^2|\mathrm{vech}(\hat{\Sigma}-\Sigma)|_\infty\right\}}.
\end{aligned}$$

Consider the following event $E = \{|\mathrm{vech}(\hat{\Sigma}-\Sigma)|_\infty < 1/(2s\vee N)\}$. Under Assumption 3.1 by Theorem A.1 and Babii, Ghysels, and Striaukas (2022a), Theorem 3.1

$$\begin{aligned}
\Pr(E^c) &\leq \Pr\left(\max_{i\in[N],j\in[p]}\left|\frac{1}{\sqrt{N}T}\sum_{t=1}^{T}\{x_{i,t,j}-\mathbb{E}[x_{i,t,j}]\}\right| \geq \frac{1}{2s\vee N}\right) \\
&\quad + \Pr\left(\max_{1\leq j\leq k\leq p}\left|\frac{1}{NT}\sum_{i=1}^{N}\sum_{t=1}^{T}x_{i,t,j}x_{i,t,k} - \mathbb{E}[x_{i,t,j}x_{i,t,k}]\right| \geq \frac{1}{2s\vee N}\right) \\
&\lesssim p(s\vee N)^{\tilde{\kappa}}T^{1-\tilde{\kappa}}(N^{1-\tilde{\kappa}/2} + pN^{1-\tilde{\kappa}}) + p(p\vee N)e^{-cNT/(s\vee N)^2}.
\end{aligned}$$

Therefore, on the event E

$$|\hat{\alpha}-\alpha|_1/\sqrt{N} + |\hat{\beta}-\beta|_1 = |\Delta_N|_1 \lesssim (s\vee N)\lambda,$$

and whence from equation (A.7) we obtain

$$\begin{aligned}
\|\mathbf{Z}\Delta\|_{NT}^2 &\lesssim \lambda\left\{|\hat{\alpha}-\alpha|_1/\sqrt{N} + \Omega(\hat{\beta}-\beta)\right\} \\
&\lesssim \lambda|\Delta_N|_1 \leq (s\vee N)\lambda^2.
\end{aligned}$$

Suppose now that $\|\mathbf{m} - \mathbf{Z}\rho\|_{NT} > \frac{1}{2}\|\mathbf{Z}\Delta\|_{NT}$. Then, obviously,

$$\|\mathbf{Z}(\hat{\rho} - \rho)\|_{NT}^2 \leq 4\|\mathbf{m} - \mathbf{Z}\rho\|_{NT}^2.$$

Therefore, on the event E, we always have

$$\|\mathbf{Z}(\hat{\rho} - \rho)\|_{NT}^2 \lesssim (s \vee N)\lambda^2 + 4\|\mathbf{m} - \mathbf{Z}\rho\|_{NT}^2,$$

which proves the statement of the theorem. □

Proof of Theorem 4.1. By Fermat's rule, the pooled sg-LASSO estimator in equation (4) satisfies

$$\mathbf{Z}^\top(\mathbf{Z}\hat{\rho} - \mathbf{y})/NT + \lambda z^* = 0$$

for some $z^* \in \partial\Omega(\hat{\rho})$. Rearranging this expression and multiplying by $\hat{\Theta}$

$$\hat{\rho} - \rho + \hat{\Theta}\lambda z^* = \hat{\Theta}\mathbf{Z}^\top\mathbf{u}/NT + (I - \hat{\Theta}\hat{\Sigma})(\hat{\rho} - \rho) + \hat{\Theta}\mathbf{Z}^\top(\mathbf{m} - \mathbf{Z}\rho)/NT,$$

where we use $\hat{\Sigma} = \mathbf{Z}^\top\mathbf{Z}/NT$ and $\mathbf{y} = \mathbf{m} + \mathbf{u}$. Plugging λz^* from the first-order conditions and multiplying by $\sqrt{NT}$

$$\sqrt{NT}(\hat{\rho} - \rho + B) = \hat{\Theta}\mathbf{Z}^\top\mathbf{u}/\sqrt{NT} + \sqrt{NT}(I - \hat{\Theta}\hat{\Sigma})(\hat{\rho} - \rho) + \hat{\Theta}\mathbf{Z}^\top(\mathbf{m} - \mathbf{Z}\rho)/\sqrt{NT}.$$

Then for a group of regression coefficients $G \subset [p+1]$, we have

$$\begin{aligned}\sqrt{NT}(\hat{\rho}_G - \rho_G + B_G) &= \frac{1}{\sqrt{NT}}\sum_{i=1}^{N}\sum_{t=1}^{T} u_{i,t}\Theta_G z_{i,t} + \frac{1}{\sqrt{NT}}\sum_{i=1}^{N}\sum_{t=1}^{T} u_{i,t}(\hat{\Theta}_G - \Theta_G)z_{i,t} \\ &\quad + \sqrt{NT}(I - \hat{\Theta}\hat{\Sigma})_G(\hat{\rho} - \rho) + \hat{\Theta}_G\mathbf{Z}^\top(\mathbf{m} - \mathbf{Z}\rho)/\sqrt{NT} \\ &\triangleq I_{N,T} + II_{N,T} + III_{N,T} + IV_{N,T}.\end{aligned}$$

We will show that by Theorem A.1, $I_{N,T} \xrightarrow{d} N(0, \Xi_G)$ as $N, T \to \infty$. To that end, by Minkowski's inequality under Assumptions 3.1 (i) and 4.1 (ii)

$$\begin{aligned}\max_{i\in[N],j\in G}\|u_{i,t}\Theta_j z_{i,t}\|_q &\leq \max_{i\in[N],j\in G}\sum_{k=1}^{p+1}\|u_{i,t}z_{i,t,k}\Theta_{j,k}\|_q \\ &\leq \|\Theta_G\|_\infty \max_{i\in[N],j\in G,k\in[p+1]}\|u_{i,t}z_{i,t,k}\|_q = O(1).\end{aligned}$$

Lastly, under Assumption 4.1 (i), for every $i, N \in \mathbf{N}$,

$$\begin{aligned}\lim_{T\to\infty}\mathrm{Var}(u_{i,t}\Theta_G z_{i,t}) &= \lim_{T\to\infty}\Theta_G\mathrm{Var}(u_{i,t}z_{i,t})\Theta_G^\top \\ &\lesssim \lim_{T\to\infty}\Theta_G\Sigma\Theta_G = (\Theta_G^\top)_G < \infty\end{aligned}$$

since groups have a fixed size. In conjunction with Assumption 3.1 (ii), this verifies conditions of Theorem A.1 and shows that $I_{N,T} \xrightarrow{d} N(0, \Xi_G)$.

Next,

$$|II_{N,T}| \leq \|\hat{\Theta}_G - \Theta_G\|_\infty \left| \frac{1}{\sqrt{NT}} \sum_{i=1}^{N} \sum_{t=1}^{T} u_{i,t} z_{i,t} \right|_\infty$$
$$= O_P\left(\frac{Sp^{1/\kappa}}{(NT)^{1-1/\kappa}} \vee S\sqrt{\frac{\log p}{NT}} \right) O_P\left(\frac{p^{1/\kappa}}{(NT)^{1/2-1/\kappa}} \vee \sqrt{\log p} \right) = o_P(1),$$

where we use Proposition A.1 and Theorem A.1. Similarly by Proposition A.1 and Corollary 3.1

$$|III_{N,T}| \leq \sqrt{NT} \max_{j \in G} |(I - \hat{\Theta}\hat{\Sigma})_j|_\infty |\hat{\rho} - \rho|_1$$
$$= O_P\left(\frac{p^{1/\kappa}}{(NT)^{1/2-1/\kappa}} \vee \sqrt{\log p} \right) O_P\left(\frac{sp^{1/\kappa}}{(NT)^{1-1/\kappa}} \vee s\sqrt{\frac{\log p}{NT}} \right) = o_P(1).$$

Lastly, by the Cauchy-Schwartz inequality

$$|IV_{N,T}|_\infty \leq \max_{j \in G} |\mathbf{Z}\hat{\Theta}_j^\top|_2 \|\mathbf{m} - \mathbf{Z}\rho\|_{NT} = \max_{j \in G} \sqrt{\hat{\Theta}_j^\top \hat{\Sigma} \hat{\Theta}_j} o_P(1)$$
$$\leq \|\hat{\Theta}_G\|_\infty \sqrt{|\text{vech}(\hat{\Sigma})|_\infty} o_P(1) = o_P(1),$$

where the second line follows under Assumption 4.1 (v), and the last by Proposition A.1 and Theorem A.1 under maintained assumptions. □

Proposition A.1. *Suppose that Assumptions 3.1, 3.2, 3.3, 3.4, and 4.1 are satisfied for each nodewise regression $j \in G$. Then if $S^\kappa p(NT)^{1-\kappa} \to 0$ and $S^2 \log p / NT \to 0$*

$$\|\hat{\Theta}_G - \Theta_G\|_\infty = O_P\left(\frac{Sp^{1/\kappa}}{(NT)^{1-1/\kappa}} \vee S\sqrt{\frac{\log p}{NT}} \right)$$

and

$$\max_{j \in G} |(I - \hat{\Theta}\hat{\Sigma})_j|_\infty = O_P\left(\frac{p^{1/\kappa}}{(NT)^{1-1/\kappa}} \vee \sqrt{\frac{\log p}{NT}} \right).$$

Proof. The proof is similar to the proof of Babii, Ghysels, and Striaukas (2022a), Propositions A.1.2 and A.1.3. □

B Concentration and moment inequalities

In this section we present a suitable for us Rosenthal's moment inequality for dependent data and a new Fuk-Nagaev concentration inequality for panel data reflecting the concentration jointly over N and T.

For a random vector $\xi_{i,t} = (\xi_{i,t,1}, \dots, \xi_{i,t,p}) \in \mathbf{R}^p$, let $\tau_k^{(i,j)}$ denote the τ-mixing coefficient of $\xi_{i,t,j}$. The following result describes a Fuk-Nagaev concentration inequality for panel data. It is worth mentioning that the inequality does not follow from Babii, Ghysels, and Striaukas (2022a) and is of independent interest for the high-dimensional panel data.[9]

Theorem A.1. *Let $\{\xi_{i,t} : i \in [N], t \in [T]\}$ be an array of centered random vectors in $\mathbf{R}^p$ such that $(\xi_{i,1}, \dots, \xi_{i,T})$ are independent over i and (i) $\max_{i\in[N],t\in[T],j\in[p]} \|\xi_{i,t,j}\|_q = O(1)$ for some $q > 2$; (ii) $\max_{i\in[N],j\in[p]} \tau_k^{(i,j)} = O(k^{-a})$ for some $a > (q-1)/(q-2)$. Then for every $u > 0$*

$$\Pr\left(\left|\sum_{i=1}^N \sum_{t=1}^T \xi_{i,t}\right|_\infty > u\right) \leq c_1 pNTu^{-\kappa} + 4pe^{-c_2 u^2/NT}$$

for some universal constants $c_1, c_2 > 0$ and $\kappa = ((a+1)q-1)/(a+q-1)$.

Proof of Theorem A.1. Suppose first that $p = 1$. For $a \in \mathbf{R}$ with some abuse of notation, let $[[a]]$ denote its integer part. For each $i \in [N]$, split the partial sum into blocks with at most $J \in \mathbf{N}$ summands

$$\begin{aligned} V_{i,k} &= \xi_{i,(k-1)J+1} + \cdots + \xi_{i,kJ}, \qquad k = 1, 2, \dots, [[T/J]] \\ V_{i,[[T/J]]+1} &= \xi_{i,[[T/J]]J+1} + \cdots + \xi_{i,T}, \end{aligned}$$

where we set $V_{i,[[T/J]]+1} = 0$ if $[[T/J]]J = T$. Let $\{U_{i,t} : i \in [N], t \in [T]\}$ be i.i.d. random variables uniformly distributed on $(0,1)$ and independent of $\{\xi_{i,t} : i \in [N], t \in [T]\}$. Put $\mathcal{M}_{i,t} = \sigma(V_{i,1}, \dots, V_{i,t-2})$ for every $t \geq 3$. For each $i \in [N]$, if $t = 1, 2$, set $V_{i,t}^* = V_{i,t}$, while if $t \geq 3$, then by Dedecker and Prieur (2004), Lemma 5, there exist random variables $V_{i,t}^* =_d V_{i,t}$ such that

1. $V_{i,t}^*$ is $\mathcal{M}_{i,t} \vee \sigma(V_{i,t}) \vee \sigma(U_{i,t})$-measurable.
2. $V_{i,t}^* \perp\!\!\!\perp (V_{i,1}, \dots, V_{i,t-2})$.
3. $\|V_{i,t} - V_{i,t}^*\|_1 = \tau(\mathcal{M}_{i,t}, V_{i,t})$.

Property 1. implies that there exists a measurable function f_i such that

$$V_{i,t}^* = f_i(V_{i,t}, V_{i,t-2}, \dots, V_{i,1}, U_{i,t}).$$

[9] The direct application of the time series Fuk-Nagaev inequality of Babii, Ghysels, and Striaukas (2022a) leads to inferior concentration results for panel data.

Property 2. implies that $(V^*_{i,2t})_{t\geq 1}$ and $(V^*_{i,2t-1})_{t\geq 1}$ are sequences of independent random variables for every $i \in [N]$. Moreover, $\{V^*_{i,2t} : i \in [N], t \geq 1\}$ and $\{V^*_{i,2t-1} : i \in [N], t \geq 1\}$ are sequences of independent random variables since $\{\xi_{i,t} : \ t \in [T]\}$ are independent over $i \in [N]$.

Decompose

$$\begin{aligned}\left|\sum_{i=1}^{N}\sum_{t=1}^{T}\xi_{i,t}\right| &\leq \left|\sum_{i=1}^{N}\sum_{t\geq 1}V^*_{i,2t}\right| + \left|\sum_{i=1}^{N}\sum_{t\geq 1}V^*_{i,2t-1}\right| + \sum_{i=1}^{N}\sum_{t=3}^{[[T/J]]+1}\left|V_{i,t} - V^*_{i,t}\right| \\ &\triangleq I + II + III.\end{aligned}$$

By Fuk and Nagaev (1971), Corollary 4 for independent data there exist constants $c_1, c_2 > 0$ such that

$$\begin{aligned}\Pr(I > u/3) &\leq c_1 u^{-q}\sum_{i=1}^{N}\sum_{t\geq 1}\mathbb{E}|V^*_{i,2t}|^q + 2\exp\left(-\frac{c_2u^2}{\sum_{i=1}^{N}\sum_{t\geq 1}\mathrm{Var}(V^*_{i,2t})}\right) \\ &\leq c_1 u^{-q}\sum_{i=1}^{N}\sum_{t\geq 1}\mathbb{E}|V_{i,2t}|^q + 2\exp\left(-\frac{c_2u^2}{NT}\right),\end{aligned}$$

where we use $V^*_{i,t} =_d V_{i,t}$ and $\sum_{i=1}^{N}\sum_{t\geq 1}\mathrm{Var}(V_{i,2t}) = O(T)$, which follows from Babii, Ghysels, and Striaukas (2022a), Lemma A.1.2 under assumptions (i) and (ii). Similarly,

$$\Pr(II > u/3) \leq c_1 u^{-q}\sum_{i=1}^{N}\sum_{t\geq 1}\mathbb{E}|V_{i,2t}|^q + 2\exp\left(-\frac{c_2u^2}{NT}\right).$$

Finally, since $\mathcal{M}_{i,t}$ and $V_{i,t}$ are separated by $J+1$ lags of $\xi_{i,t}$, we have $\tau(\mathcal{M}_{i,t}, V_{i,t}) \leq J\tau_J^{(i,j)}(J+1)$. By Markov's inequality and property 3., this gives

$$\Pr(III > u/3) \leq \frac{3}{u}\sum_{i=1}^{N}\sum_{t=3}^{[[T/J]]+1}\|V_{i,t} - V^*_{i,t}\|_1 \leq \frac{3NT}{u}\max_{i\in[N]}\tau_{J+1}^{(i,1)}.$$

Combining all estimates together under (i)-(ii)

$$\begin{aligned}\Pr\left(\left|\sum_{i=1}^{N}\sum_{t=1}^{T}\xi_{i,t}\right| > u\right) &\leq \Pr(I > u/3) + \Pr(II > u/3) + \Pr(III > u/3) \\ &\leq c_1 u^{-q} N\sum_{i=1}^{N}\sum_{t\geq 1}\|V_{i,t}\|_q^q + 4e^{-c_2u^2/NT} + \frac{3NT}{u}\max_{i\in[N]}\tau_{J+1}^{(i,1)} \\ &\leq c_1 u^{-q} J^{q-1}NT + \frac{3NT}{u}(J+1)^{-a} + 4e^{-c_2u^2/NT}\end{aligned}$$

for some constants $c_1, c_2 > 0$. To balance the first two terms, we shall choose the length of blocks $J \sim u^{\frac{q-1}{q+a-1}}$, in which case we get

$$\Pr\left(\left|\sum_{i=1}^{N}\sum_{t=1}^{T}\xi_{i,t}\right| > u\right) \leq c_1 NTu^{-\kappa} + 4e^{-c_2 u^2/NT}$$

for some $c_1, c_2 > 0$. Finally, for $p > 1$, the result follows by the union bound. □

It follows from Theorem A.1 that there exists $C > 0$ such that for every $\delta \in (0,1)$

$$\Pr\left(\left|\frac{1}{NT}\sum_{t=1}^{T}\sum_{i=1}^{N}\xi_{i,t}\right|_{\infty} \leq C\left(\frac{p}{\delta(NT)^{\kappa-1}}\right)^{1/\kappa} \vee \sqrt{\frac{\log(p/\delta)}{NT}}\right) \geq 1-\delta.$$

Note that the inequality reflects the concentration jointly over N and T and that tails and persistence play an important role through the mixing-tails exponent κ. The inequality is a key technical tool that allows us to handle panel data with heavier than Gaussian tails and non-negligible T and N. It is worth mentioning that the concentration over N is also influenced by the weak dependence, which probably can be relaxed with a sharper proof technique. However, for geometrically ergodic processes, e.g., for stationary $AR(p)$, we have $\kappa \approx q$, in which case the time series dependence does not influence the concentration at all.

Let $(\xi_t)_{t\in\mathbf{N}}$ be a real-valued stochastic process, and let Q_t denote the generalized inverse of the tail function $x \mapsto \Pr(|\xi_t| \geq x)$. Let $\xi \in \mathbf{R}$ be a random variable corresponding to $(\xi_t)_{t\in\mathbf{Z}}$ such that $Q \geq \sup_{t\in\mathbf{N}} Q_t$, where Q is a generalized inverse of $x \mapsto \Pr(|\xi| \geq x)$. The following Rosenthal's moment inequality for τ-dependent sequences follows from Dedecker and Prieur (2004); see also Dedecker and Doukhan (2003).

Theorem A.2. *Let $(\xi_t)_{t\in\mathbf{N}}$ be a centered stochastic process such that (i) there exists $q > 2$ such that $\|\xi\|_q < \infty$, where $\xi \in \mathbf{R}$ corresponds to $(\xi_t)_{t\in\mathbf{N}}$; (ii) the τ-mixing coefficients are $\tau_{k-1} \leq ck^{-a}, \forall k \geq 1$ for some universal constants $c > 0$ and $a > (q(r-2)+1)/(q-r)$. Then for every $r \in [2, q)$*

$$\mathbb{E}\left|\sum_{t=1}^{T}\xi_t\right|^r \leq c_{q,r}\left(T^{r/2}\|\xi\|_q^{qr/2(q-1)} + T\|\xi\|_q^{q(r-1)/(q-1)}\right),$$

where the constant $c_{q,r}$ depends only on q and r.

Proof. Let G be the inverse of $x \mapsto \int_0^x Q(u)\mathrm{d}u$ and put $H(u) = \sum_{k=0}^{\infty} \mathbb{1}_{2u<\tau_k}$, where $(\tau_k)_{k\in\mathbf{N}}$ are τ-mixing coefficients of $(\xi_t)_{t\in\mathbf{N}}$. Note that for every $q \geq 1$,

$$\int_0^{\|\xi\|_1} |Q \circ G(u)|^{q-1}\mathrm{d}u = \int_0^1 Q^q(v)\mathrm{d}v = \|\xi\|_q^q.$$

Then by Hölder's inequality

$$\int_0^{\|\xi\|_1} |H(u)Q \circ G(u)|^{r-1} \mathrm{d}u \leq \left(\int_0^{\|\xi\|_1} H^{(q-1)(r-1)/(q-r)}(u) \mathrm{d}u \right)^{\frac{q-1}{q-r}} \|\xi\|_q^{q(r-1)/(q-1)}$$

Note also that for some constant $C_{q,r}$ that depends only on q and r we have

$$\begin{aligned}
\int_0^{\|\xi\|_1} H^{(q-1)(r-1)/(q-r)}(u) \mathrm{d}u &\leq (1 \vee s_{q,r}) \int_0^{\|\xi\|_1} \sum_{k=0}^{\infty} (k+1)^{(q-1)(r-1)/(q-r)-1} \mathbb{1}_{2u<\tau_k} \mathrm{d}u \\
&\leq 0.5(1 \vee s_{q,r}) \sum_{k=0}^{\infty} (k+1)^{(q-1)(r-1)/(q-r)-1} \tau_k \\
&\leq 0.5c(1 \vee s_{q,r}) \sum_{k=1}^{\infty} k^{(q-1)(r-1)/(q-r)-1-a} \\
&\leq C_{q,r}
\end{aligned}$$

where we use the fact that $H^s(u) = \sum_{k=0}^{\infty}((k+1)^s - k^s)\mathbb{1}_{2u<\tau_k}$, $(k+1)^s - k^s \leq (1 \vee s)(k+1)^{s-1}$ with $s = s_{q,r} = (q-1)(r-1)/(q-r)$, and the series converges since $a > (q(r-2)+1)/(q-r)$. Combining these estimates

$$\int_0^{\|\xi\|_1} |H(u)Q \circ G(u)|^{r-1} \mathrm{d}u \leq C_{q,r}^{\frac{q-1}{q-r}} \|\xi\|_q^{q(r-1)/(q-1)}. \tag{A.10}$$

By Dedecker and Prieur (2004), Corollary 1, for some constant $c_r > 0$ that depends only on r

$$\begin{aligned}
\mathbb{E}\left| \sum_{t=1}^{T} \xi_t \right|^r &\leq c_r \left\{ \left(T \int_0^{\|\xi\|_1} H(u)Q \circ G(u) \mathrm{d}u \right)^{r/2} + T \int_0^{\|\xi\|_1} |H(u)Q \circ G(u)|^{r-1} \mathrm{d}u \right\} \\
&\leq c_r \left\{ T^{r/2} \left(C_{q,r}^{\frac{q-1}{q-2}} \|\xi\|_q^{q/(q-1)} \right)^{r/2} + T C_{q,r}^{\frac{q-1}{q-r}} \|\xi\|_q^{q(r-1)/(q-1)} \right\} \\
&\leq c_{q,r} \left(T^{r/2} \|\xi\|_q^{qr/2(q-1)} + T \|\xi\|_q^{q(r-1)/(q-1)} \right),
\end{aligned}$$

where the second line follows by equation (A.10) and $c_{q,r} > 0$ depends only on q and r. □

C Large N and T central limit theorem

For a double sequence $\{a_{N,T} : N, T \in \mathbf{N}\}$, we use $\lim_{N,T\to\infty} a_{N,T}$ to denote the limit when $N, T \to \infty$ jointly and $\max_{N,T\in\mathbf{N}} a_{N,T} = \max\{a_{N,T} : N \in \mathbf{N}, T \in \mathbf{N}\}$. The following central limit theorem holds for panel data consisting of τ-mixing processes that may change over N and T.

Theorem A.1. *Let $\{\xi_{N,T,i,t} : i \in \mathbf{N}, t \in \mathbf{Z}\}$ be an array of centered random vectors in $\mathbf{R}^p$ such that for each N, T, and i, $\{\xi_{N,T,i,t} : t \in \mathbf{Z}\}$ is a stationary process in $\mathbf{R}^p$ and $\{(\xi_{N,T,i,1}, \ldots, \xi_{N,T,i,T}) : i \in \mathbf{N}\}$ are independent arrays in $\mathbf{R}^p \times \mathbf{R}^T$ satisfying (i) for some $q > 2$, $\max_{i\in[N],j\in[p]} \|\xi_{N,T,i,t,j}\|_q = O(1)$; (ii) for all N, T, i, j, the τ-mixing coefficients of $\{\xi_{N,T,i,t,j} : t \in \mathbf{Z}\}$ satisfy $\tau_{k-1} \leq ck^{-a}, \forall k \geq 1$ for some universal constants $c > 0$ and $a > (q-1)/(q-2) \vee (q\delta+1)/(q-2-\delta)$ with $q > 2+\delta$ and $\delta > 0$; (iii) for every $i, N \in \mathbf{N}$, $\lim_{T\to\infty} \mathrm{Var}(\xi_{N,T,i,t}) < \infty$. Then*

$$\frac{1}{\sqrt{NT}} \sum_{i=1}^{N} \sum_{t=1}^{T} \xi_{N,T,i,t} \xrightarrow{\mathrm{d}} N(0, \Xi) \qquad as \qquad N, T \to \infty,$$

where $\Xi = \lim_{N,T\to\infty} \frac{1}{N} \sum_{i=1}^{N} \mathrm{Var}\left(\frac{1}{\sqrt{T}} \sum_{t=1}^{T} \xi_{N,T,i,t}\right)$ is a finite matrix, assumed to be a positive definite.

Proof. By the Cramér-Wold device, see Billingsley (1995), Theorem 29.4,

$$\frac{1}{\sqrt{NT}} \sum_{i=1}^{N} \sum_{t=1}^{T} \xi_{N,T,i,t} \xrightarrow{\mathrm{d}} N(0, \Xi) \qquad \text{as} \qquad N, T \to \infty$$

in $\mathbf{R}^p$ if and only if for every $z \in \mathbf{R}^p$, the following weak convergence holds in $\mathbf{R}$

$$z^\top \left(\frac{1}{\sqrt{NT}} \sum_{i=1}^{N} \sum_{t=1}^{T} \xi_{N,T,i,t} \right) \xrightarrow{\mathrm{d}} N(0, z^\top \Xi z) \qquad \text{as} \qquad N, T \to \infty.$$

Note that under maintained assumptions, for each N, T and $z \in \mathbf{R}^p$,

$$z^\top \left(\frac{1}{\sqrt{NT}} \sum_{i=1}^{N} \sum_{t=1}^{T} \xi_{N,T,i,t} \right) = \sum_{i=1}^{N} z^\top \left(\frac{1}{\sqrt{NT}} \sum_{t=1}^{T} \xi_{N,T,i,t} \right)$$

is a sum of N independent zero-mean random variables. By independence and stationarity, the variance of this sum is

$$\begin{aligned} \sigma^2_{N,T,z} &\triangleq \frac{1}{N} \sum_{i=1}^{N} \mathrm{Var}\left(\frac{1}{\sqrt{T}} \sum_{t=1}^{T} z^\top \xi_{N,T,i,t} \right) \\ &= \frac{1}{N} \sum_{i=1}^{N} \left\{ \mathrm{Var}(z^\top \xi_{N,T,i,t}) + 2 \sum_{k=1}^{T-1} \left(1 - \frac{k}{T}\right) \mathrm{Cov}(z^\top \xi_{N,T,i,0}, z^\top \xi_{N,T,i,k}) \right\}. \end{aligned}$$

If we show that the limit in the parentheses exists for every $i, N \in \mathbf{N}$, then the joint limit of $\sigma^2_{N,T,z}$ as $N, T \to \infty$ is the same as the sequential limit

$$\lim_{N\to\infty} \lim_{T\to\infty} \frac{1}{N} \sum_{i=1}^{N} \left\{ \mathrm{Var}(z^\top \xi_{N,T,i,t}) + 2 \sum_{k=1}^{T-1} \left(1 - \frac{k}{T}\right) \mathrm{Cov}(z^\top \xi_{N,T,i,0}, z^\top \xi_{N,T,i,k}) \right\};$$

see Apostol (1974), Theorem 8.39. By Babii, Ghysels, and Striaukas (2022a), Lemma A.1.1, for every $k \geq 1$

$$|\mathrm{Cov}(z^\top \xi_{N,T,i,0}, z^\top \xi_{N,T,i,k})| \leq \tau_k^{\frac{q-2}{q-1}} \|z^\top \xi_{N,T,i,0}\|_q^{q/(q-1)} = O(k^{-a}),$$

where the second inequality follows under (i)-(ii). Moreover, $\sum_{k=1}^\infty k^{-a} < \infty$ under (ii). Therefore, by Lebesgue's dominated convergence theorem, for every $i, N \in \mathbf{N}$,

$$\lim_{T\to\infty} \sum_{k=1}^{T-1} \left(1 - \frac{k}{T}\right) \mathrm{Cov}(z^\top \xi_{N,T,i,0}, z^\top \xi_{N,T,i,k}) < \infty,$$

and whence under (ii)

$$\lim_{N,T\to\infty} \sigma_{N,T}^2 = \lim_{N,T\to\infty} \frac{1}{N} \sum_{i=1}^N \mathrm{Var}\left(\frac{1}{\sqrt{T}} \sum_{t=1}^T z^\top \xi_{N,T,i,t}\right) = z^\top \Xi z < \infty.$$

The statement of the theorem follows by the central limit theorem for independent random variables, provided that the following Lyapunov condition holds

$$\lim_{N,T\to\infty} \frac{1}{(NT)^{1+\delta/2}} \sum_{i=1}^N \mathbb{E}\left|\sum_{t=1}^T z^\top \xi_{N,T,i,t}\right|^{2+\delta} = 0;$$

see Billingsley (1995), Theorem 27.3 and Phillips and Moon (1999), Theorem 2.

By Theorem A.2, for some $c_{q,\delta}$ that depends only on q and δ,

$$\mathbb{E}\left|\sum_{t=1}^T z^\top \xi_{N,T,i,t}\right|^{2+\delta} \leq c_{q,\delta} \left\{T^{1+\delta/2} \|z^\top \xi_{N,T,i,t}\|_q^{q(1+\delta/2)/(q-1)} + T \|z^\top \xi_{N,T,i,t}\|_q^{q(1+\delta)/(q-1)}\right\}.$$

Therefore, the Lyapunov condition holds under (i). □

ONLINE APPENDIX

OA.1 Data description

OA.1.1 Firm-level data

The full list of firm-level data is provided in Table 2. We also add two daily firm-specific stock market predictor variables: stock returns and a realized variance measure, which is defined as the rolling sample variance over the previous 60 days (i.e. 60-day historical volatility).

OA.1.1.1 Firm sample selection

We select a sample of firms based on data availability. First, we remove all firms from I/B/E/S which have missing values in earnings time series. Next, we retain firms that we can match with CRSP dataset. Finally, we keep firms that we can match with the RavenPack dataset.

OA.1.1.2 Firm-specific text data

We create a link table of RavenPack ID and PERMNO identifiers which enables us to merge I/B/E/S and CRSP data with firm-specific textual analysis generated data from RavenPack. The latter is a rich dataset that contains intra-daily news information about firms. There are several editions of the dataset; in our analysis, we use the Dow Jones (DJ) and Press Release (PR) editions. The former contains relevant information from Dow Jones Newswires, regional editions of the Wall Street Journal, Barron's and MarketWatch. The PR edition contains news data, obtained from various press releases and regulatory disclosures, on a daily basis from a variety of newswires and press release distribution networks, including exclusive content from PRNewswire, Canadian News Wire, Regulatory News Service, and others. The DJ edition sample starts at 1^{st} of January, 2000, and PR edition data starts at 17^{th} of January, 2004.

We construct our news-based firm-level covariates by filtering only highly relevant news stories. More precisely, for each firm and each day, we filter out news that has the *Relevance Score* (REL) larger or equal to 75, as is suggested by the RavenPack News Analytics guide and used by practitioners; see for example Kolanovic and Krishnamachari (2017). REL is a score between 0 and 100 which indicates how strongly a news story is linked with a particular firm. A score of zero means that the

entity is vaguely mentioned in the news story, while 100 means the opposite. A score of 75 is regarded as a significantly relevant news story. After applying the REL filter, we apply a novelty of the news filter by using the *Event Novelty Score* (ENS); we keep data entries that have a score of 100. Like REL, ENS is a score between 0 and 100. It indicates the novelty of a news story within a 24-hour time window. A score of 100 means that a news story was not already covered by earlier announced news, while a subsequently published news story score on a related event is discounted, and therefore its scores are less than 100. Therefore, with this filter, we consider only novel news stories. We focus on *five sentiment indices* that are available in both DJ and PR editions. They are as follows.

Event Sentiment Score (ESS), for a given firm, represents the strength of the news measured using surveys of financial expert ratings for firm-specific events. The score value ranges between 0 and 100 — values above (below) 50 classify the news as being positive (negative), 50 being neutral.

Aggregate Event Sentiment (AES) represents the ratio of positive events reported on a firm compared to the total count of events measured over a rolling 91-day window in a particular news edition (DJ or PR). An event with ESS > 50 is counted as a positive entry while ESS < 50 is negative. Neutral news (ESS $= 50$) and news that does not receive an ESS score do not enter into the AES computation. As ESS, the score values are between 0 and 100.

Aggregate Event Volume (AEV) represents the count of events for a firm over the last 91 days within a certain edition. As in the AES case, news that receives a non-neutral ESS score is counted and therefore accumulates positive and negative news.

Composite Sentiment Score (CSS) represents the news sentiment of a given news story by combining various sentiment analysis techniques. The direction of the score is determined by looking at emotionally charged words and phrases and by matching stories typically rated by experts as having short-term positive or negative share price impact. The strength of the scores is determined by intra-day price reactions modeled empirically using tick data from approximately 100 large-cap stocks. As for ESS and AES, the score takes values between 0 and 100, 50 being the neutral.

News Impact Projections (NIP) represents the degree of impact a news flash has on the market over the following two-hour period. The algorithm produces scores

to accurately predict a relative volatility — defined as scaled volatility by the average of volatilities of large-cap firms used in the test set — of each stock price measured within two hours following the news. Tick data are used to train the algorithm and produce scores, which take values between 0 and 100, 50 representing zero impact news.

For each firm and each day with firm-specific news, we compute the average value of the specific sentiment score. In this way, we aggregate across editions and groups, where the latter is defined as a collection of related news. We then map the indices that take values between 0 and 100 onto $[-1, 1]$. Specifically, let $x_i \in \{\text{ESS}, \text{AES}, \text{CSS}, \text{NIP}\}$ be the average score value for a particular day and firm. We map $x_i \mapsto \bar{x}_i \in [-1, 1]$ by computing $\bar{x}_i = (x_i - 50)/50$. For days with no news, we impute zero values. Note that series are centered around zero, where zero value means zero impact news. Therefore, imputing zeros is the same as assuming that no news on a given day implies zero impact news, which we believe is a reasonable assumption.

	Ticker	Firm name	PERMNO	RavenPack ID
1	MMM	3M	22592	03B8CF
2	ABT	Abbott labs	20482	520632
3	AUD	Automatic data processing	44644	66ECFD
4	ADTN	Adtran	80791	9E98F2
5	AEIS	Advanced energy industries	82547	1D943E
6	AMG	Affiliated managers group	85593	30E01D
7	AKST	A K steel holding	80303	41588B
8	ATI	Allegheny technologies	43123	D1173F
9	AB	AllianceBernstein holding l.p.	75278	CB138D
10	ALL	Allstate corp.	79323	E1C16B
11	AMZN	Amazon.com	84788	0157B1
12	AMD	Advanced micro devices	61241	69345C
13	DOX	Amdocs ltd.	86144	45D153
14	AMKR	Amkor technology	86047	5C8D61
15	APH	Amphenol corp.	84769	BB07E4
16	AAPL	Apple	14593	D8442A
17	ADM	Archer daniels midland	10516	2B7A40
18	ARNC	Arconic	24643	EC821B
19	ATTA	AT&T	66093	251988
20	AVY	Avery dennison corp.	44601	662682
21	BHI	Baker hughes	75034	940C3D
22	BAC	Bank of america corp.	59408	990AD0
23	BAX	Baxter international inc.	27887	1FAF22
24	BBT	BB&T corp.	71563	1A3E1B
25	BDX	Becton dickinson & co.	39642	873DB9
26	BBBY	Bed bath & beyond inc.	77659	9B71A7
27	BHE	Benchmark electronics inc.	76224	6CF43C
28	BA	Boeing co.	19561	55438C
29	BK	Bank of new york mellon corp.	49656	EF5BED
30	BWA	BorgWarner inc.	79545	1791E7
31	BP	BP plc	29890	2D469F
32	EAT	Brinker international inc.	23297	732449
33	BMY	Bristol-Myers squibb co.	19393	94637C
34	BRKS	Brooks automation inc.	81241	FC01C0
35	CA	CA technologies inc.	25778	76DE40
36	COG	Cabot oil & gas corp.	76082	388E00
37	CDN	Cadence design systems inc.	11403	CC6FF5
38	COF	Capital one financial corp.	81055	055018
39	CRR	Carbo ceramics inc.	83366	8B66CE
40	CSL	Carlisle cos.	27334	9548BB
41	CCL	Carnival corporation & plc	75154	067779
42	CERN	Cerner corp.	10909	9743E5
43	CHRW	C.H. robinson worldwide inc.	85459	C659EB
44	SCHW	Charles schwab corp.	75186	D33D8C
45	CHKP	Check point software technologies ltd.	83639	531EF1
46	CHV	Chevron corp.	14541	D54E62
47	CI	CIGNA corp.	64186	86A1B9
48	CTAS	Cintas corp.	23660	BFAEB4
49	CLX	Clorox co.	46578	719477
50	KO	Coca-Cola co.	11308	EEA6B3
51	CGNX	Cognex corp.	75654	709AED
52	COLM	Columbia sportswear co.	85863	5D0337
53	CMA	Comerica inc.	25081	8CF6DD
54	CRK	Comstock resources inc.	11644	4D72C8
55	CAG	ConAgra foods inc.	56274	FA40E2
56	STZ	Constellation brands inc.	69796	1D1B07
57	CVG	Convergys corp.	86305	914819

58	COST	Costco wholesale corp.	87055	B8EF97
59	CCI	Crown castle international corp.	86339	275300
60	DHR	Danaher corp.	49680	E124EB
61	DRI	Darden restaurants inc.	81655	9BBFA5
62	DVA	DaVita inc.	82307	EFD406
63	DO	Diamond offshore drilling inc.	82298	331BD2
64	D	Dominion resources inc.	64936	977A1E
65	DOV	Dover corp.	25953	636639
66	DOW	Dow chemical co.	20626	523A06
67	DHI	D.R. horton inc.	77661	06EF42
68	EMN	Eastman chemical co.	80080	D4070C
69	EBAY	eBay inc.	86356	972356
70	EOG	EOG resources inc.	75825	A43906
71	EL	Estee lauder cos. inc.	82642	14ED2B
72	ETH	Ethan allen interiors inc.	79037	65CF8E
73	ETFC	E*TRADE financial corp.	83862	28DEFA
74	XOM	Exxon mobil corp.	11850	E70531
75	FII	Federated investors inc.	86102	73C9E2
76	FDX	FedEx corp.	60628	6844D2
77	FITB	Fifth third bancorp	34746	8377DB
78	FISV	Fiserv inc.	10696	190B91
79	FLEX	Flex ltd.	80329	B4E00D
80	F	Ford motor co.	25785	A6213D
81	FWRD	Forward air corp.	79841	10943B
82	BEN	Franklin resources inc.	37584	5B6C11
83	GE	General electric co.	12060	1921DD
84	GIS	General mills inc.	17144	9CA619
85	GNTX	Gentex corp.	38659	CC339B
86	HAL	Halliburton Co.	23819	2B49F4
87	HLIT	Harmonic inc.	81621	DD9E41
88	HIG	Hartford financial services group inc.	82775	766047
89	HAS	Hasbro inc.	52978	AA98ED
90	HLX	Helix energy solutions group inc.	85168	6DD6BA
91	HP	Helmerich & payne inc.	32707	1DE526
92	HSY	Hershey co.	16600	9F03CF
93	HES	Hess corp.	28484	D0909F
94	HON	Honeywell international inc.	10145	FF6644
95	JBHT	J.B. Hunt transport services Inc.	42877	72DF04
96	HBAN	Huntington bancshares inc.	42906	C9E107
97	IBM	IBM corp.	12490	8D4486
98	IEX	IDEX corp.	75591	E8B21D
99	IR	Ingersoll-Rand plc	12431	5A6336
100	IDTI	Integrated device technology inc.	44506	8A957F
101	INTC	Intel corp.	59328	17EDA5
102	IP	International paper co.	21573	8E0E32
103	IIN	ITT corp.	12570	726EEA
104	JAKK	Jakks pacific inc.	83520	5363A2
105	JNJ	Johnson & johnson	22111	A6828A
106	JPM	JPMorgan chase & co.	47896	619882
107	K	Kellogg co.	26825	9AF3DC
108	KMB	Kimberly-Clark corp.	17750	3DE4D1
109	KNGT	Knight transportation inc.	80987	ED9576
110	LSTR	Landstar system inc.	78981	FD4E8D
111	LSCC	Lattice semiconductor corp.	75854	8303CD
112	LLY	Eli lilly & co.	50876	F30508
113	LFUS	Littelfuse inc.	77918	D06755
114	LNC	Lincoln national corp.	49015	5C7601
115	LMT	Lockheed martin corp.	21178	96F126

116	MTB	M&T bank corp.	35554	D1AE3B
117	MANH	Manhattan associates inc.	85992	031025
118	MAN	ManpowerGroup inc.	75285	C0200F
119	MAR	Marriott international inc.	85913	385DD4
120	MMC	Marsh & mcLennan cos.	45751	9B5968
121	MCD	McDonald's corp.	43449	954E30
122	MCK	McKesson corp.	81061	4A5C8D
123	MDU	MDU resources group inc.	23835	135B09
124	MRK	Merck & co. inc.	22752	1EBF8D
125	MTOR	Meritor inc	85349	00326E
126	MTG	MGIC investment corp.	76804	E28F22
127	MGM	MGM resorts international	11891	8E8E6E
128	MCHP	Microchip technology inc.	78987	CDFCC9
129	MU	Micron technology inc.	53613	49BBBC
130	MSFT	Microsoft corp.	10107	228D42
131	MOT	Motorola solutions inc.	22779	E49AA3
132	MSM	MSC industrial direct co.	82777	74E288
133	MUR	Murphy oil corp.	28345	949625
134	NBR	Nabors industries ltd.	29102	E4E3B7
135	NOI	National oilwell varco inc.	84032	5D02B7
136	NYT	New york times co.	47466	875F41
137	NFX	Newfield exploration co.	79915	9C1A1F
138	NEM	Newmont mining corp.	21207	911AB8
139	NKE	NIKE inc.	57665	D64C6D
140	NBL	Noble energy inc.	61815	704DAE
141	NOK	Nokia corp.	87128	C12ED9
142	NOC	Northrop grumman corp.	24766	FC1B7B
143	NTRS	Northern trust corp.	58246	3CCC90
144	NUE	NuCor corp.	34817	986AF6
145	ODEP	Office depot inc.	75573	B66928
146	ONB	Old national bancorp	12068	D8760C
147	OMC	Omnicom group inc.	30681	C8257F
148	OTEX	Open text corp.	82833	34E891
149	ORCL	Oracle corp.	10104	D6489C
150	ORBK	Orbotech ltd.	78527	290820
151	PCAR	Paccar inc.	60506	ACF77B
152	PRXL	Parexel international corp.	82607	EF8072
153	PH	Parker hannifin corp.	41355	6B5379
154	PTEN	Patterson-uti energy inc.	79857	57356F
155	PBCT	People's united financial inc.	12073	449A26
156	PEP	PepsiCo inc.	13856	013528
157	PFE	Pfizer inc.	21936	267718
158	PIR	Pier 1 imports inc.	51692	170A6F
159	PXD	Pioneer natural resources co.	75241	2920D5
160	PNCF	PNC financial services group inc.	60442	61B81B
161	POT	Potash corporation of saskatchewan inc.	75844	FFBF74
162	PPG	PPG industries inc.	22509	39FB23
163	PX	Praxair inc.	77768	285175
164	PG	Procter & gamble co.	18163	2E61CC
165	PTC	PTC inc.	75912	D437C3
166	PHM	PulteGroup inc.	54148	7D5FD6
167	QCOM	Qualcomm inc.	77178	CFF15D
168	DGX	Quest diagnostics inc.	84373	5F9CE3
169	RL	Ralph lauren corp.	85072	D69D42
170	RTN	Raytheon co.	24942	1981BF
171	RF	Regions financial corp.	35044	73C521
172	RCII	Rent-a-center inc.	81222	C4FBDC
173	RMD	ResMed inc.	81736	434F38

174	RHI	Robert half international inc.	52230	A4D173
175	RDC	Rowan cos. inc.	45495	3FFA00
176	RCL	Royal caribbean cruises ltd.	79145	751A74
177	RPM	RPM international inc.	65307	F5D059
178	RRD	RR R.R. donnelley & sons co.	38682	0BE0AE
179	SLB	Schlumberger ltd. n.v.	14277	164D72
180	SCTT	Scotts miracle-gro co.	77300	F3FCC3
181	SM	SM st. mary land & exploration co.	78170	6A3C35
182	SONC	Sonic corp.	76568	80D368
183	SO	Southern co.	18411	147C38
184	LUV	Southwest airlines co.	58683	E866D2
185	SWK	Stanley black & decker inc.	43350	CE1002
186	STT	State street corp.	72726	5BC2F4
187	TGNA	TEGNA inc.	47941	D6EAA3
188	TXN	Texas instruments inc.	15579	39BFF6
189	TMK	Torchmark corp.	62308	E90C84
190	TRV	The travelers companies inc.	59459	E206B0
191	TBI	TrueBlue inc.	83671	9D5D35
192	TUP	Tupperware brands corp.	83462	2B0AF4
193	TYC	Tyco international plc	45356	99333F
194	TSN	Tyson foods inc.	77730	AD1ACF
195	X	United states Steel corp.	76644	4E2D94
196	UNH	UnitedHealth group inc.	92655	205AD5
197	VIAV	Viavi solutions inc.	79879	E592F0
198	GWW	W.W. grainger inc.	52695	6EB9DA
199	WDR	Waddell & reed financial inc.	85931	2F24A5
200	WBA	Walgreens boots alliance inc.	19502	FACF19
201	DIS	Walt disney co.	26403	A18D3C
202	WAT	Waters corp.	82651	1F9D90
203	WBS	Webster financial corp.	10932	B5766D
204	WFC	Wells fargo & co.	38703	E8846E
205	WERN	Werner enterprises inc.	10397	D78BF1
206	WABC	Westamerica bancorp	82107	622037
207	WDC	Western digital corp.	66384	CE96E7
208	WHR	Whirlpool corp.	25419	BDD12C
209	WFM	Whole foods market inc.	77281	319E7D
210	XLNX	Xilinx inc.	76201	373E85

Table OA.1: Final list of firms — The table contains the information about the full list of firms: tickers, firm names, CRSP PERMNO code and RavenPack ID. Tickers and firm names are taken as of June, 2017. PERMNO and RavenPack ID columns are used to match firms and firm news data.